N° d'ordre :
N° de série :

République Algérienne Démocratique et Populaire

Ministère de l'Enseignement Supérieur et de la Recherche Scientifique

Mémoire de Fin d'Études

Présenté à

L'Université Echahid Hamma Lakhdar d'El Oued

Faculté de la Technologie

Département de Génie Electrique

En vue de l'obtention du diplôme de

MASTER ACADEMIQUE

En Commande Electrique

Présenté par

HENKA Ali - BOUDINA Safa - HARICHA Naima

Thème

Speed Control of quadcopter motors for a dynamic Stability

Soutenu le 15/06/2022. Devant le jury composé de:

Dr. CHERIF Hakima	Président
Dr. LABIOD Chouaib	Rapporteur
Dr. MAHMOUDI Abdelkader	Examinateur

Année Universitaire 2021/2022

Dedication

I dedicate this humble work to My parents, who have always been there for me Since my childhood, I could not Achieving this success without their support May God protect them.

I dedicate this work to the one who put her fingertips from the first step in the project KASMI TOURKIA

For my sister who has not left me since the beginning of work BOUDINA SAFA

I dedicate to you this humble work without you I could not have reached and to my dear brother and my Dr: LABIOD CHOUAIB for his support during my studies

To my brothers: HOCINE, A. KADER, A. ASSALAM

To my dear sister: AICHA, ASSIA, ZOUHRA

To everyone who helped me from far or near

HENKA Ali

Dedication

I dedicate this humble work to:

My dad BOUDINA BELGACEM and mom MOUMEN SAAD MASSOUDA, who always supported me since my childhood, without their support, I would not have been able to complete this work, allah keep them safe.

To my brothers and friends who have supported me in overcoming many obstacles and difficulties.

To all my dear teachers who did not hesitate to extend a helping hand to me.

BOUDINA SAFA

Dedication

To the gleaming handles of my life, my parents.

To my sisters, to my brothers

To my best teachers for ever,

Mrs. BEKHOUCHA NASSIMA,

To all my friends.

To all those who fed me with confidence, support, and acknowledgment,

I dedicate this humble work.

Haricha Naima

Thanks

Would like to sincerely thank our research director, ***Dr. LABIOD Chouaib****, for methodological assistance, relevant advice and regular follow-up.*

We thanks extend to the members of the jury who agreed to read and judge our work.

We would also like to thank all the teachers in the electrical engineering department, especially the head of the department Dr. Messoud Hettiri.

We thank all the teachers who helped us in this work, especially:

Dr. Hakima Cherif, Dr. Nassima Bekhoucha, Dr. Gassem Abdelmalek

We would also like to thank and express we gratitude to the people who helped me directly or indirectly for the completion of this work.

Abstract

Recent years have witnessed a qualitative leap that affected all areas of life: political, social, and technological. Where are the manifestations of this development varied from one field to another, and the technology of drones obtained its significant share of this development to enter the civil field from its wide door, to have a major role in serving the humanitarian community and focusing on the vital areas that are related to the daily life of the human being for the purpose of sharing the effort with the human element and paying the risks that may be exposed to it while performing some tasks.

This work aims to speed control of quadcopter BLDC motor for dynamic stability. For this purpose, the mathematical model of the BLDC motor associated with the inverter was implemented in Simulink Matlab software, as well as for the control of speed and angle in order to ensure stability when flying.

After the modeling and simulation, we extract the data model based on experimentally testing for the mechanical and electrical data modeling in order to obtain a model closer to real machine and to obtain optimum regulator parameters more stable system in speed or angle control.

Finally, we carried out the experimental work in real-time, where the results showed the effectiveness and efficacy of the proposed control for this study.

Keywords: Brushless Motor, Speed control Dynamic stabilization of Quad-copter, Experimental test, Data modeling.

ملخص

شهدت السنوات الأخيرة نقلة نوعية مست كل مجالات الحياة: السياسية، الاجتماعية والتكنولوجية. حيث اختلفت مظاهر هذا التطور من مجال إلى آخر، وقد نالت تكنولوجيا الطائرات بدون طيار نصيبها المعتبر من هذا التطور لتدخل إلى المجال المدني من بابه الواسع، ليكون لها دور كبير في خدمة المجتمع الإنساني والتركيز على المجالات الحيوية التي ترتبط بالحياة اليومية للإنسان بغرض تقاسم الجهد مع العنصر البشري ودفع المخاطر التي قد يتعرض لها أثناء أداء بعض المهام.

يهدف هذا العمل إلى التحكم الديناميكي في محرك BLDC الخاص بالطائرة الرباعية ذاتية القيادة من أجل هذه الغاية قمنا بالنمذجة الرياضية للمحرك مع المحول العكوس وتم تنفيذ هذه النمذجة في برنامج "Simulink Matlab"، كذلك بالنسبة للتحكم في السرعة والزاوية من أجل ضمان الاستقرار عند الطيران.

بعد النمذجة والمحاكاة قمنا بالكشف التجريبي لبيانات المحرك من أجل الحصول على نموذج أكثر قربا للحقيقة، والحصول على إعدادات تحكم أكثر استقرار سواءا من أجل التحكم في السرعة أو الزاوية.

وفي الأخير قمنا بالعمل التجريبي في الوقت الحقيقي وأظهرت النتائج مدى فعالية ونجاعة التحكم المقترح من أجل هذه الدراسة.

الكلمات المفتاحية: محرك بدون مستشعرات موضع، مراقبة السرعة، الاستقرار الديناميكي للمروحية الرباعية، الاختبار التجريبي، نمذجة المعطيات.

List of Figures

List of tables

List of Acronyms

UAV	Unmanned Aerial Vehicle
VTOL	Vertical Take Off and Landing
BLDC	Brushless Direct Current Motor
PWM	Pulse Width Modulation
PI	Proportional Integral
DC	Direct Current
USB	Universal Serial Bus
ESC	Electronic Speed Controllers
RPM	Revolution Per Minute
CW	Clockwise
CCW	Counter-Clockwise
DOF	Degree OF Freedom
EMF	Electro Motive Force
PMSM	Permanent Magnet Synchronous Motor
IGBT	Insulated Gate Bipolar Transistor
GTO	Gate Turn Off

Summary

General introduction

General Introduction:

In recent years, researchers have had more interested in autonomous aerial vehicles (Unmanned Aerial Vehicles, UAV). These flying machines are also called drones (false drones). Drones are aircraft capable of flying and carrying out unmanned missions on board, traveling long distances, and taking readings in dangerous areas and thus preventing people from exposing themselves to these dangers and making extremely precise readings on thermal imaging, topographic survey, distance calculation, volume calculation, which are occupying an increasingly important place in the aeronautics and defense sectors and represent the strongest progression of the sector of the aeronautics and space industry, which is organizing to develop system technologies and define the services that can be offered among a multitude of related applications. The civilian drone market is booming. The potential of these aerial systems without a pilot on board has won over several sectors of the industry.

In fact, it involves very varied fields such as aerodynamics, signal and image processing, automatic control, mechanics, composite materials, and real-time computing among these drones, the quad-copter stands out as one of the most popular devices. Promising due to the diversity of applications for which it can be used. The mission of surveillance and observation, aerial photography, control of the state of a building difficult to access, or even the transport of goods are currently largely developed by manufacturers [1].

In this project, we are particularly interested in miniature aerial vehicles and more particularly in a quad-copter (micro helicopter with four propellers) with a system of shooting. Quad-copter drones are among the most complex flying objects because their flight dynamics are inherently nonlinear, and the variables are strongly coupled. The quad-copter has the ability to hover, which is required in some apps. The objective of this project is to studies of speed and angle control for dynamic stabilization in one axes of Quad-copter drone piloted via a microcontroller (Arduino), thus a realization of a flight controller which embeds the different sensors to manage the quad-copter autonomously[2]. Then, for stabilization of the quad-copter around the equilibrium position (hovering flight), we have developed a linear approach by a PI regulator. The remaining of the project is organized as follows:

In the first chapter, we have briefly presented the historical context associated with the appearance of rotary-wing drones. We have also seen the main types and drone architectures and their applications. In addition, we mentioned the various constraints and difficulties that can limit the applications of a drone and its reliability.

The second chapter deals with the aerodynamics of the quad-copter using mechanical and electrical model for one axes for one degree freedom of quad-copter instead of six degrees of freedom for which we add the aerodynamic forces generated by its actuators. Firstly, we presented and studied the modeling and control of a quad rotor motor, where cross studied simulations of associated BLDC motor an inverter and speed control by using MATLAB. Furthermore, we studied the modeling of BLDC with inverter and speed control system. Finally, we presented the results of Simulink for speed control[3].

The third chapter presents the data model of the BLDC motor based on experimental test for the simulation model of the mechanical and electrical system has been developed, and the real time speed and angle control has been achieved by using PI regulator. Hence, the optimum parameter K_i, Kp tested in Simulink model applied on real time controller.

Finally, we present the results of voltage, current speed and angle in real time has been presented for different situations of regulator parameters k_i, k_p. The last results approve the effectiveness and validity of realized system[4].

Chapter I: General study on quadcopter motors

I.1 Introduction:

Quadcopter is a type of remotely piloted or pre-programmed UAV, consisting of four engines that contribute to flight, guidance and stability, and we chose this type of UAV due to its most common multi-rotor design.

This first chapter provides general information about drones. Types of drones and their uses, the motor used and the principle of operation of the quadcopter in particular, with the advantages, disadvantages and configurations of the quadcopter.

I.2 Different Types of Drone:

Here is a rundown of the four main types of drones, their uses, their strengths and weaknesses:

- Multi-Rotor Drones (Bicopter, Tricopter, QuadCopter, Y4, VTail and ATail, Pentacopter, Hexacopter, Y6 Hexacopter, Octocopter, X8).
- Fixed-Wing Drones.
- Single-Rotor Drones.
- Fixed-Wing Hybrid VTOL.

I.2.1 Multi-Rotor Drones:

Multirotor systems are a subset of rotorcraft. The term rotorcraft is used in aviation to define aircraft that use rotary wings to generate lift. Rotorcraft can have one or multiple rotors. Drones using rotary systems are almost always equipped with multiple small rotors, which are necessary for their stability, hence the name multirotor systems. This four-rotor drone will be discussed in more detail later in this section. Differences between fixed-wing drones and multirotor drones are important for the different applications consumers want to use the drone for. For example, multirotor drones do not need a landing strip, make less noise than their fixedwing counterparts. [2].

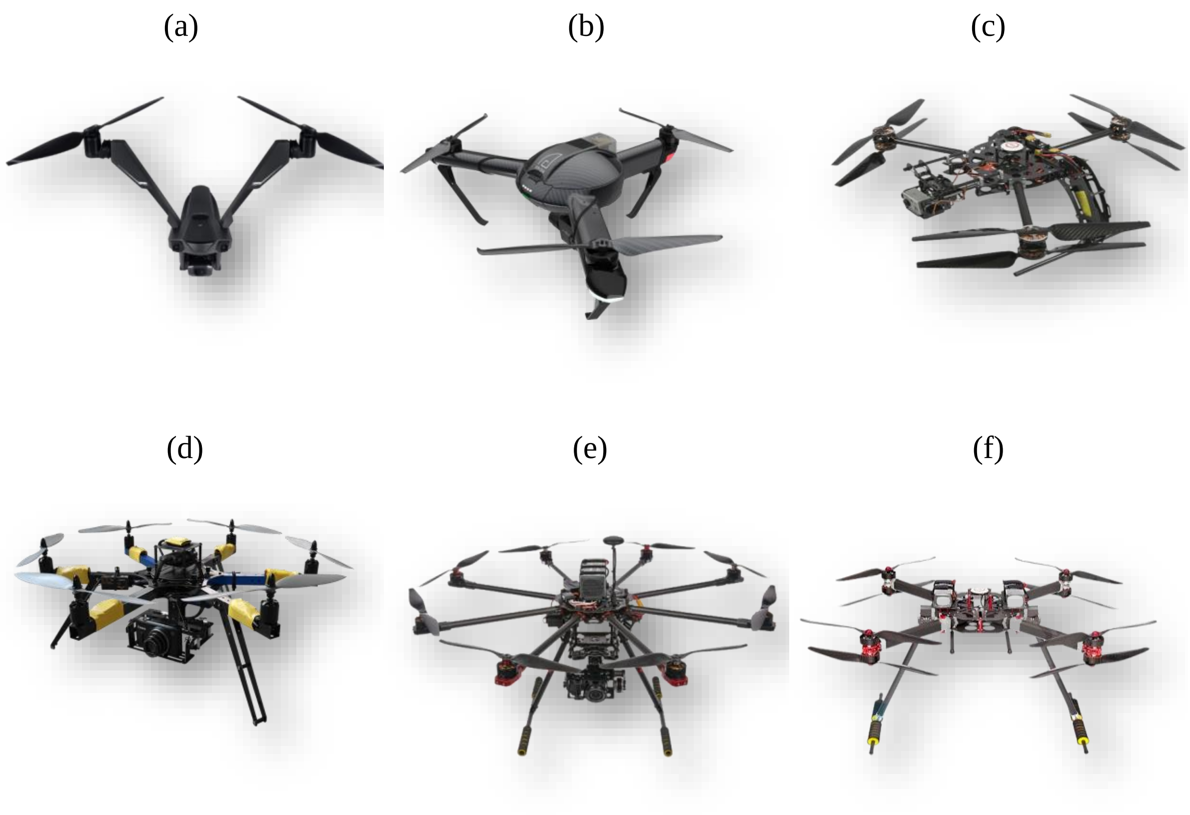

Figure I. 1: Multi-rotor drones, (a) Bicopter, (b)Tricopter , (c)Y6 Hexacopter, (d) Hexacopter, (e)Octocopter, (f) X8.

I.2.2 Fixed-Wing Drones:

Fixed-wing drones are heavier-than-air drones capable of flying with lift from its wings generated by their forward movement through the air. This makes them the suitable drones for long distance missions because of their lesser energy consumption. They can fly at higher altitudes, with virtually no obstacles, that allow them to move at a higher speed and enables them to cover a larger area in less time. They have the ability to camouflage from higher altitudes , and are normally equipped with long distance cameras. They are easy to be controlled from known flight parameters, have better aerodynamic performance with minor influence from environmental conditions, and can glide to avoid crashes. Some of their disadvantages include the need for a big space for take-off and landing, harder for a pilot to fly thus the need of more pilot training and expertise, unable to do VTOL and unable to hover, and they are expensive to build and maintain because of the material used [3].

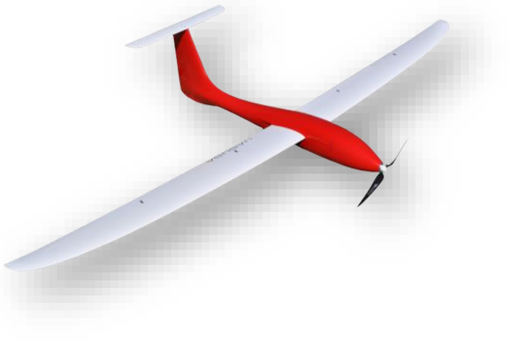

Figure I. 2: fixed-wing drones**.**

I.2.3 Single-Rotor Drones:

A single Rotor helicopter drones are having more advantages if compared with other type of drones. For sustaining more endurance, it is fixed with the gas controlled system. The Aerodynamic rules stress that, if any system is having larger rotor blades then the spin will

be less, and efficiency of the system will be more. Because of this, the single rotor helicopters are more efficient if it is compared with other kind of drones. Since single rotor helicopters are having long rotor blades, it is having more advantage in agricultural fields. The structure of single rotor helicopter is as shown in figure 3 [4].

Figure I. 3: Single-Rotor Helicopter (Source).

I.2.4 Fixed-Wing Hybrid Vtol:

The hybrid UAV use quadrotor mode for taking off and landing and fly like a plane using fixed-wing mode through the mission.

Tail sitter UAV is pointed upwards and takes-off vertically using thrusters. When it reaches the required altitude it will tilt 90 degree and fly using wings. UAV share the same principle of operation. They take-off using vertical thrusters, and when the required altitude is reached, the thrusters gently pitch forward for cruising. Considering the complexity and risk associated with these designs, a hybrid design where quadrotor and fixed wing UAV types are connected together seem to be a good intuitive choice. In this type of hybrid VToL UAVs the simplicity and safety can be significantly improved by eliminating tilt-rotors [5].

Figure I. 4: Fixed-wing hybrid VTOL.

I.3 Classification of used motors:

I.3.1 Brush motor:

DC motor make up of a fixed stator made of two permanent magnets, and a rotor wound with coils and mounted on bearings such that it is free to turn. The rotor consists of a crossbar wound with wire to form a coil but with the direction of winding changed from one side of the crossbar to the other. By Ampere’s Law, current passing through each set of windings generates a magnetic flux distribution, creating a pair of electromagnets. Because the wire is wound in opposite directions on each side, the electromagnets have opposite polarities [6].

Figure I. 5: Examples of brush DC motors of various types and frame sizes. The largest motor shown here has a diameter of three inches.

I.3.2 Brushless motors:

Brushless motors used in quadcopter offer more power, speed and longer run times than conventional brushed motors of the same size. The superior power and efficiency of the brushless motor make them the ideal choice for high performance quadcopter.

Figure I. 6: Brushless motor.

They are a bit similar to normal DC motors in the way that coils and magnets are used to drive the shaft. Though the brushless motors do not have a brush which takes care of switching the power direction in the coils. This is why they are called brushless. Instead, the brushless motors have three coils on the inner (center) of the motor, which is fixed to the mounting (stator). The outer side (rotor) contains a numb er of magnets mounted to a cylinder that is attached to the rotating shaft. So the coils are fixed. This means wires can go directly to the coils. Therefore there is no need for a brush [7].

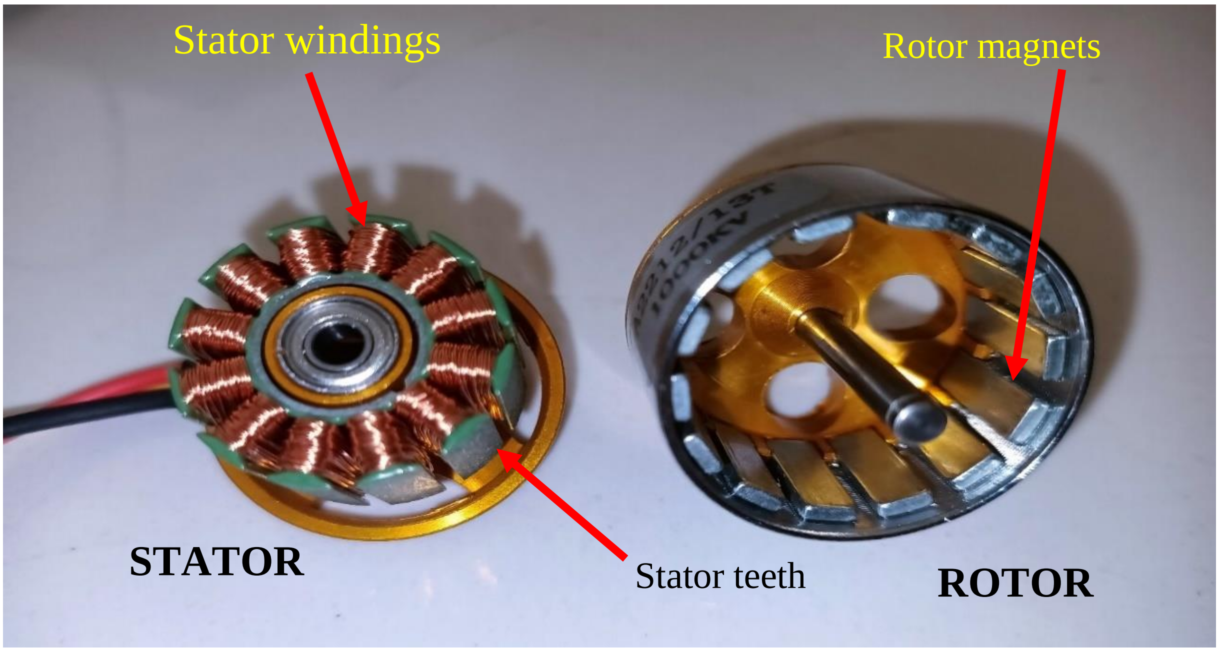

Figure I. 7: Stator and rotor of brushless motor

I.4 Quadcopter Applications:

UAVs are utilised for different application, some of these applications are discussed here.

Drones in agriculture:

Comparion of light reflectance in near infrared an dvisible wavelengths is particularly important because it is related to vegetative biomass and/or growth vigor in crops. It therefore allows differences between vegetation at different locations in a field to be quantified greatly enhancing the ability to use aerial imaging-based computational methods for vegetation analysis. Additional information can be derived by targeting the transition between visible to near infrared reflectance (the so-called "red edge"), or by using specific, relatively narrow wavelength ranges that respond uniquely to specific changes in vegetation [8].

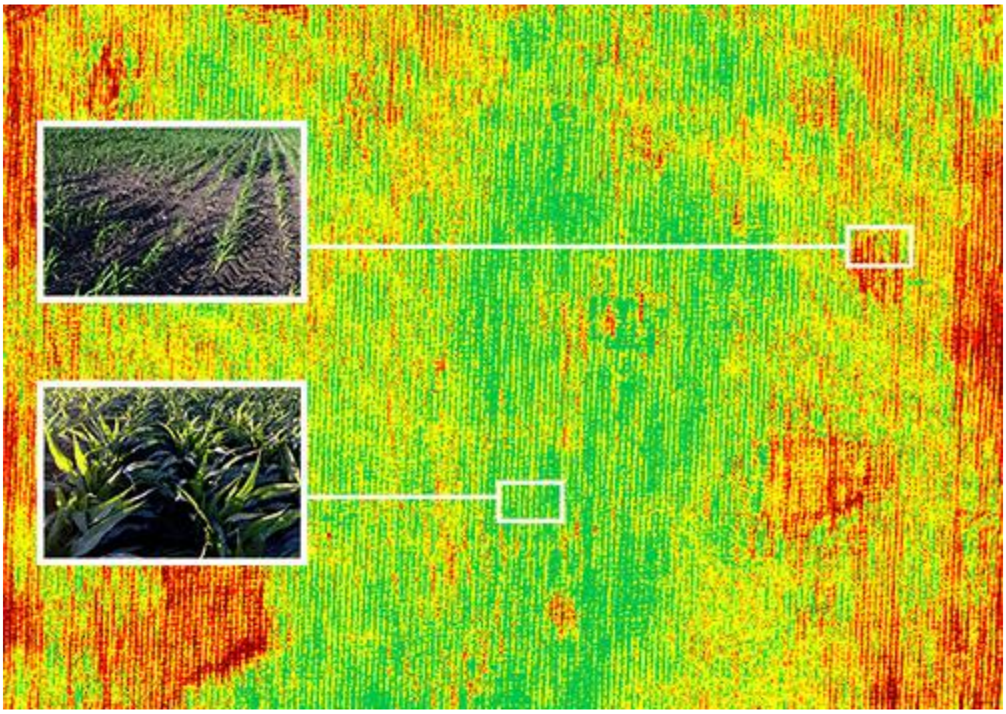

Figure I. 8: A normalized difference vegetation index map of a corn field, derived from high spatial resolution aerial images, demonstrating the power of fine spatial resolution to assist in the identification of the causes of variability within a crop field.

- **Military drone:**

In the military, drones have the potential to reduce costs and risks to personnel can be used in lethal surveillance and targeted killings compared to using manned aircraft.

Artificial intelligence plays a key role in military drones, which has made such drones able to differentiate between civilians and the targets. The discourse is on the ability of the AI machines to be able to execute tasks with ethical considerations [9].

Figure I. 9: Military Drones.

- **Environmental protection:**

Although drones are considered as a vital part of military missions, they are also being increasingly used for performing environmental actions, such as managing national parks and agricultural lands, tracking wildlife in different areas, observing the effects of climate change, and monitoring the biodiversity of different ecosystems from rainforests to the oceans . These drones can be used for recognition and investigation of natural disasters including forest fires، avalanches on mountains, etc [10].

Figure I. 10: Drones and wildlife monitoring.

- **Mailing and delivery:**

Package delivery is one of the most enticing UAV applications supported by major courier companies for quick, cost-effective and efficient transportation of packages that weigh less than a UAV maximum bearing load. Where the adoption of UAVs is increasing rapidly due to the growing trend of online ordering in congested cities, especially in the retail sector [11].

Figure I. 11: Drone delivery service.

- **Using a UAV for exploration:**

Unmanned Air Vehicles are light, fast and can be designed to carry the essentialaid equipment. Along with that unmanned vehicles can be used to perform criticaloperations in areas where human life cannot be risked [12].

Figure I. 12: Anti-shock drone to explore difficult areas.

- **Films & television industries:**

Drones are now being used to capture footage that requires expensive helicopters and cranes. Fast-paced action and sci-fi scenes are filmed by aerial drones, thus making cinematography easier. These autonomous flying devices are also used in real estate and sports photography. Furthermore, it is considering the use of drones for collecting footage and information in live broadcasts[13].

Figure I. 13: Drone for cinematography.

- **Drones in Search and Rescue Operations:**

Drones provide rapid solutions in support of communications coverage of rescue operations, can provide disaster warnings and assist with accelerating rescue and recovery operations when the communications networks are not serving. Drones also have the capability to carry medical supplies to hard-to-reach areas. In certain circumstances (e.g., poisonous gas infiltration and searching for missing persons), drones can support the role of accelerating these operations [14].

Figure I. 14: Search and rescue by Drones.

I.5 Design and Components of Quadcopter:

Aircraft design the design challenges of an aircraft rely on the type of application, which specifies the coverage area, maximum altitude, speed, climb rate, flight time or endurance, and stability. All the specifications are prone to vary contingent on applications and the environmental effects. Higher altitude specifies a large coverage area and improves survivability although maximum altitude is limited by the aviation regulations. Climb rate also increases the survivability. Flight time is strictly dependent on the type of operation and aerodynamic design of aircraft. The main components of aircraft subsystems are [15]:

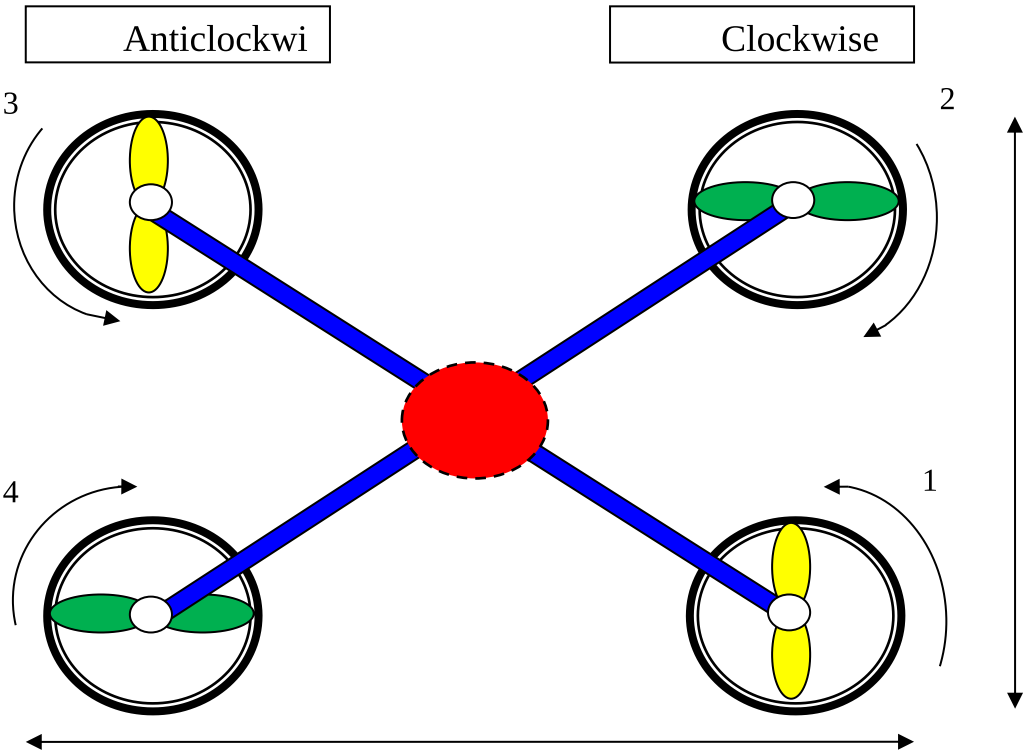

Figure I. 15: Design and rotation direction of the quadcopter.

- ✓ **Chassis:** the structure of the drone which all componentry is fixed to. The chassis design is a trade-off between strength (especially when additional weights such as cameras are attached) and additional weight, which will require longer propellers and stronger motors to lift.
- ✓ **4 Propellers:** principally effect load the drone can carry the speed it can fly and the speed it can manoeuvre. The length can be modified; longer propellers can achieve greater lift at a lower rpm but take longer to speed up/slow down. Shorter propellers can change speed quicker and thus are more manoeuvrable; however they require a higher rotational speed to achieve the same power as longer blades. This causes excess motor strain and thus reduces motor life span. A more aggressive pitch will allow quicker movement but reduced hovering efficiency.
- ✓ **4 Motors:** 1 per propeller, drone motors are rated in "kV" units which equates to the number of revolutions per minute it can achieve when a voltage of 1 volt is supplied to the motor with no load. A faster motor spin will give more flight power, but requires more power from the battery resulting in a decreased flight time.
- ✓ **4 Electronic Speed Controllers (ESC):** provides a controlled current to each motor to produce the correct spin speed and direction.
- ✓ **Flight Controller/arduino:** the onboard computer which interprets incoming signals sent from the pilot and sends corresponding inputs to the ESC to control the quadcopter.
- ✓ **Radio Receiver:** receives the control signals from the pilot.
- ✓ **Battery:** generally lithium polymer batteries are used due to high power density and ability to recharge [13].

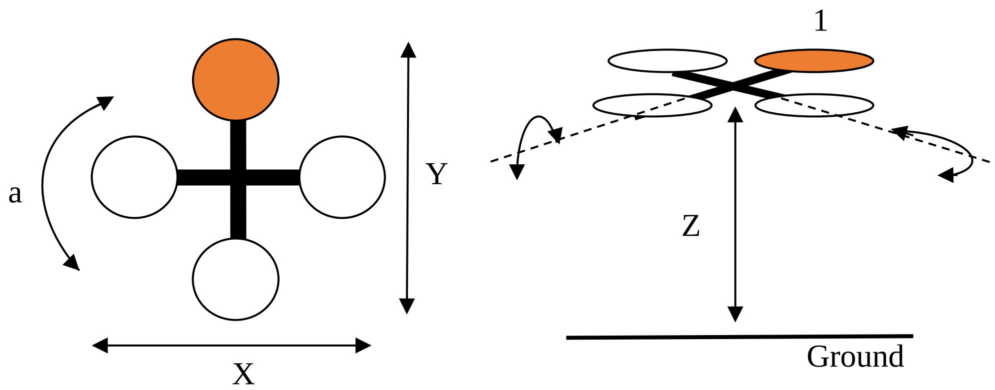

Figure I. 16: the six degrees of freedom of the quadcopter.

I.6 Structure and Working Principle of A Quadcopter :

Quadcopters use 2 sets of identical fixed pitched propellers; 2 clockwise (CW) and 2 counter-clockwise (CCW). These use variation of RPM to control lift and torque. Control of vehicle motion is achieved by altering the rotation rate of one or more rotor discs, thereby changing its torque load and thrust/lift characteristics. The front and the rear propellers rotate counterclockwise, while the left and the right ones turn clockwise. This configuration of opposite pairs directions re-moves the need for a tail rotor (needed instead in the standard helicopter structure). Figure I.18 shows the structure model in hovering condition, where all the propellers have the same speed.

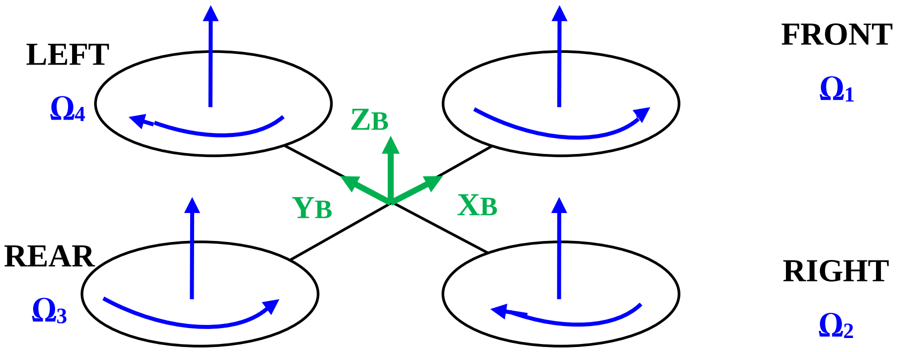

Figure I. 17: The quadcopter structure model in hovering condition.

In Figure I.17 a fixed-body B-frame of quadcopter is shown (XB, YB, ZB). Also the angular speed of the propellers is represented. In addition to the name of the velocity variable, for each propeller, two arrows are drawn: the curved one represents the direction of rotation, the other one represents the velocity. This last vector always points upwards hence it doesn't follow the right hand rule (for clockwise rotation) because it also models a vertical thrust and it would be confusing to have two speed vectors pointing upwards and the other two pointing downwards. All four propellers rotate at the same speed which is represented as Ω [rad s-1] to counterbalance the acceleration due to gravity.

Even though the quadcopter has 6 DOF, it is equipped just with four propellers. Thanks to its structure, four best controllable variables can be chosen related to the four basic movements which allow the quadcoper to reach a certain height and attitude. It follows the description of these basic movements:

• Throttle (U1 [N]) - increasing (or decreasing) all the propeller speeds by the same amount. It leads to a vertical force which raises or lowers the quadcopter. If the quadcopter is in horizontal position, the vertical direction of the inertial frame coincide. Otherwise the provided thrust generates both vertical and horizontal accelerations in the inertial frame.

• Roll (U2 [N m]) - increasing (or decreasing) the left propeller speed and by decreasing (or increasing) the right one. It leads to a torque with respect to the XB axis (Fig. I.17) which makes the quadcopter turn. The overall vertical thrust is the same as in hovering, hence this leads only to a roll angle acceleration (in first approximation).

• Pitch (U3 [N m]) - similar to the roll and is provided by increasing (or decreasing) the rear propeller speed and by decreasing (or increasing) the front one. It leads to a torque with respect to the YB axis (Fig. I.17) which makes the quadcopter turn. The overall vertical thrust is the same as in hovering, hence this leads only to a pitch angle acceleration (in first approximation).

• Yaw (U4 [N m]) - increasing (or decreasing) the frontrear propellers' speed and by decreasing (or increasing) that of the left-right couple. It leads to a torque with respect to the ZB axis (Fig. I.17) which makes the quadcopter turn. The yaw movement is generated thanks to the fact that the left-right propellers rotate clockwise while the front-rear ones rotate counter clockwise. When the overall torque is unbalanced, the quadcopter turns on itself around ZB. The total vertical thrust is the same as in hovering, hence this leads only to a yaw angle acceleration (in first approximation) [16].

I.7 Advantages and Disadvantages of Quadcopter:

Advantages:

- ♦ Extremely high spatial resolution.
- ♦ Potential for high temporal resolution.
- ♦ Insensitivity to cloud cover.
- ♦ Potential for three-dimensional drone image generation.
- ♦ Shallow learning curve of drone users.
- ♦ Relatively low price of drone imagery.
- ♦ Data acquisition decentralization.
- ♦ Enhanced monitoring of illegal activities.
- ♦ Access to otherwise inaccessible areas.
- ♦ Potential environmental benefits.
- ♦ Potential social and institutional strengthening of communities.
- ♦ Control of data acquisition and ownership would lie in community members' hands[15].

Disadvantages:

- Small payload.
- Low spectral resolution.
- Poor geometric and radiometric performance.
- Low software automation.
- Sensitivity to atmospheric conditions.
- Short flight endurance.
- Possibility of collisions.
- Potential problems for repairs and maintenance.
- Dependence on external assistance and funding.
- Ambiguous or cumbersome regulatory environments for flying small drones.
- Safety & security issues.
- Potentiel social impacts [17].

I.8 Conclusion:

Quadcopter is a special kind of vehicle, which can be implemented in different applications. In this paper, basic principles of quadcopter design as well as current applications are represented. In the future applications, quadcopter could be used for a variety of new policing functions. Quadcopter could be used for safety inspections, perimeter patrols around prisons and thermal imaging to check for cannabis being grown in roof lofts and other not easy to access locations. The police could use them to capture number plates of speeding drivers, for detecting theft from cash machines, railway monitoring, combat fly-posting, fly-tipping, abandoned vehicles, waste management. Future research will be in field of search and rescue. In future, an effort will be directed to development of a system for defining evacuation/safe path in case of natural disasters and accidents. The system will consists of quadcopter, which is equipped with a camera to capture different terrain (land or water) and a processing unit for processing the recorded condition, which is placed on the vehicle/vessel or in form of handheld device. In addition to the situations of natural disasters and accidents it is possible to use this system in cases of climatic changes that affect the safety and health of the population or in cases where it is endangering the functionality of different economic systems.

Chapter II: Modeling and control of a quadcopter motor

II.1 Introduction:

Electrical motors are consuming almost half of all the electrical energy used in the world. Most of the times motors found in all appliances are either single phase induction motors or brushed dc motors, which have low efficiency and high maintenance. Single phase induction motors are less efficient because of the ohmic loss in the rotor. But this type of loss can be reduced in Brushless DC (BLDC) motor due to the absence of brush and mechanical commutation [18].

In this chapter, we will study the modeling and control of a quad-rotor motor, where cross study simulations of speed and angle control for the dynamic stabilization in one degree freedom of quad-copter using MATLAB.

II.2 Modeling of BLDC motor:

II.2.1 Structure of BLDC motor:

The BLDC motor is a permanent magnet synchronous motor that uses position detectors and an inverter to control the armature currents. The BLDC motor is sometimes referred to as an inside-out DC motor because its armature is in the stator and the magnets are on the rotor and its operating characteristics resemble those of a DC motor. Instead of using a mechanical commentator as in the convention DC motor. The BLCD motor employs electronic commutation which makes it a virtually maintenance-free motor [19].

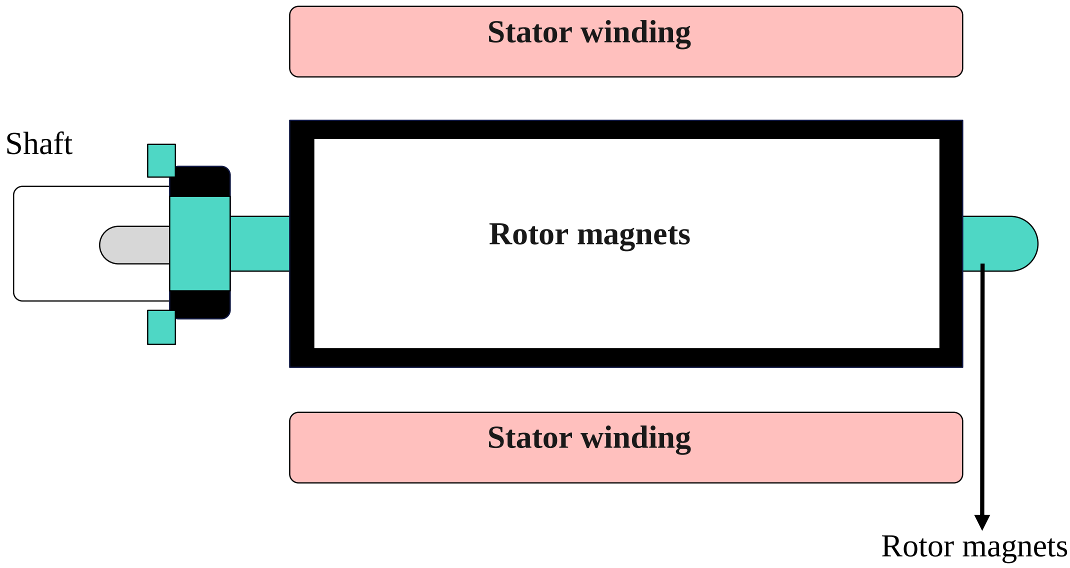

Figure II. 1: Structure of BLDC motor [20].

The sinusoidal motor needs a high-resolution position sensor because the rotor position must be known at every time instant for optimal operation. It also requires more complex software and hardware. The trapezoidal motor is a more attractive alternative for most applications due to its simplicity. Lower price and higher efficiency. The remaining part of this text discusses trapezoidal BLDC motors only [19].

BLDC motors exist in many different configurations but the three-phase motor is the most common type due to its efficiency and low torque ripple. This type of motor also offers a good compromise between precise control and number of power electronic devices needed to control the stator currents. Position detection is usually implemented using three Hall-effect sensors that detect the presentence of small magnets that are attached to the motor shaft [19].

II.3.1 Driving principle of Brushless direct current motors:

The basic driving principle of the BLDC motor is to change the phase windings, which should be excited according to the position of permanent magnet on the rotor for producing a continuous torque. To implement this function, information on the rotor magnet position is indispensable. The position sensing is commonly achieved with Hall effect sensors.

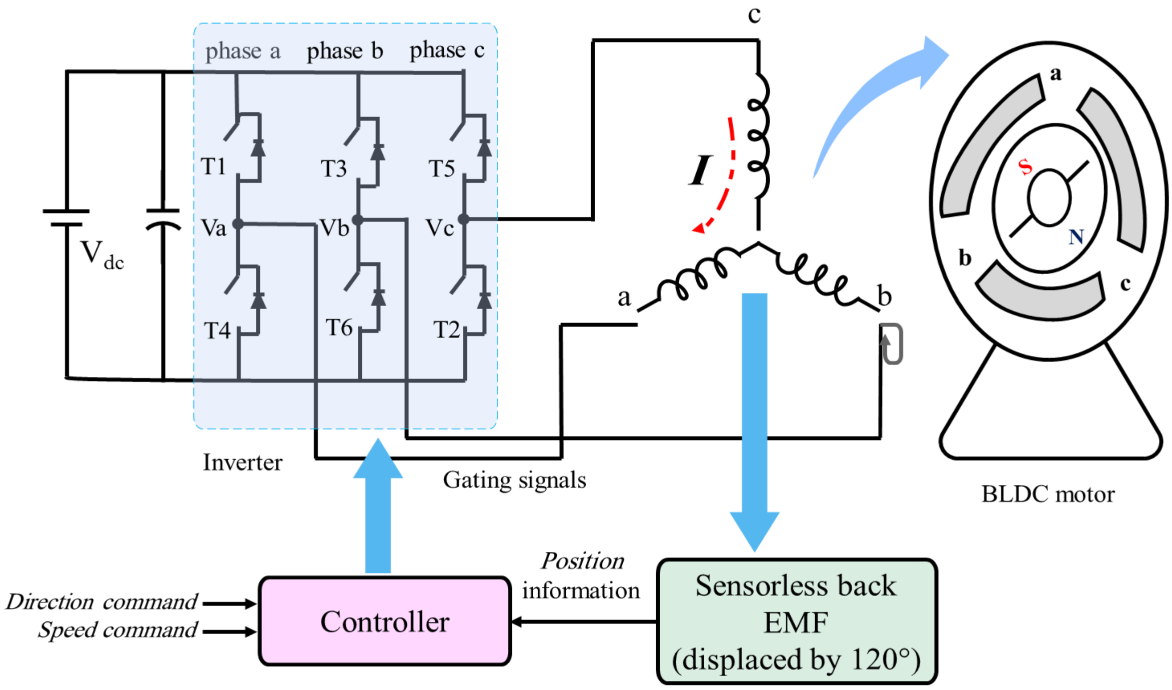

Figure II. 2: BLCD motor drive system.

A two-pole three-phase Y-connected BLDC motor drive system is shown in Figure II.3.Three Hall effect sensors are displaced from each other by 120 electrical degrees on the stator to detect the magnetic field flux produced from the rotor magnets. Three output signals of Hall effect sensors enable us to recognize the rotor position divided into six different sections. Accordingly, a basic drive (often called six-step drive) to complete one electrical cycle consists of six different sections [21].

II.3.2 Modeling of brushless motor:

In this section, we will derive the mathematical model of a three-phase BLDC motor. The model of a BLDC motor is similar to that of a PMSM due to their structural similarity [22].

$$v_{abcs} = R_s i_{abcs} + \frac{d\lambda_{abcs}}{dt} \tag{II.1}$$

Where the stator voltage $v_{abcs} = [v_{as} v_{bs} v_{cs}]^T$, the stator current $i_{abcs} = [i_{as} i_{bs} i_{cs}]^T$the stator flux linkage$\boldsymbol{\lambda_{abcs}} = [\lambda_{as} \lambda_{bs} \lambda_{cs}]^T$, and the stator resistance

$$R_s = \begin{bmatrix} R_s & 0 & 0 \\ 0 & R_s & 0 \\ 0 & 0 & R_s \end{bmatrix}. \tag{II.2}$$

The flux linkage $\boldsymbol{\lambda_{abcs}}$ of the stator windings consists of $\boldsymbol{\lambda_{abcs(s)}}$ due to the stator currents i_{abcs} and $\boldsymbol{\lambda_{abcs(f)}}$ due to the permanent magnet as

$$\boldsymbol{\lambda_{abcs}} = \boldsymbol{\lambda_{abcs(s)}} + \boldsymbol{\lambda_{abcs(f)}} \tag{II.3}$$

Substituting Eq. (II.3) into Eq. (II.1) gives the following stator voltage equation[22].

$$v_{abcs} = \boldsymbol{R}_s \boldsymbol{i}_{abcs} + \frac{d\lambda_{abcs}}{dt} = \boldsymbol{R}_s \boldsymbol{i}_{abcs} + \frac{d\lambda_{abcs}}{dt} + \boldsymbol{e}_{abcs} \tag{II.4}$$

where the back-EMF due to the magnet flux is expressed as $\boldsymbol{e}_{abcs} = d\lambda_{abcs(f)}/dt$ and is also given as **:**

$$e_{abcs} = \begin{bmatrix} e_{as} \\ e_{bs} \\ e_{cs} \end{bmatrix} = \omega_m = \begin{bmatrix} \lambda_{asf} \\ \lambda_{bsf} \\ \lambda_{csf} \end{bmatrix} = \omega_m \lambda_f \begin{bmatrix} f(\theta_r) \\ f(\theta_r - 120^\circ) \\ f(\theta_r - 240^\circ) \end{bmatrix} \tag{II. 5}$$

Where $\lambda_f\left(N\phi_f\right)$is the amount of the magnet flux $\phi_f$linking N turns of the stator windings, $f(\theta_r)$is a unit function representing the waveform of the back-EMF andθ_r is the rotor position.

The unit function for the trapezoidal back-EMF waveform of a BLDC motor can be expressed as**:**

$$f(\theta_r) = \begin{cases} 6\theta_r/\pi & (0 \le \theta_r < \pi/6) \\ 1 & (0 \le \theta_r < \pi/6) \\ -6\theta_r/\pi & (0 \le \theta_r < \pi/6) \\ -1 & (0 \le \theta_r < \pi/6) \\ 6\theta_r/\pi - 12 & (0 \le \theta_r < \pi/6) \end{cases} \tag{II .6}$$

The stator flux linkage $\boldsymbol{\lambda}_{abcs(s)}$due to the stator currents is given by

$$\lambda_{abcs(s)} = L_s i_{abcs} = \begin{bmatrix} L_{aa} & L_{ab} & L_{ac} \\ L_{ba} & L_{bb} & L_{bc} \\ L_{ca} & L_{cb} & L_{cc} \end{bmatrix} \begin{bmatrix} i_{as} \\ i_{bs} \\ i_{cs} \end{bmatrix} \tag{II. 7}$$

As can be seen in Section 4.1.1, for symmetry three-phase windings, the self-inductances are all the same and the mutual-inductances are all the same as in the following [22].

$$L_{aa} = L_{bb} = L_{cc} = L_s = L_{is} = L_m \tag{II. 8}$$

$$L_{ab} = L_{ac} = L_{ba} = L_{bc} = L_{ca} = L_{cb} = -\frac{1}{2} L_m = M \tag{II. 9}$$

here, since $i_{as} + i_{bs} + i_{cs} = 0$, the mid-term of Eq. (II.9) is reduced as

$$\frac{d}{dt}[L_s i_{as} + M_{bs} i_{cs} + M_{cs}] = \frac{d}{dt}[L_s i_{as} - M i_{as}] \tag{II. 10}$$

where $L_{\alpha\beta}\left(= \lambda/i_\beta\right)$expresses the winding inductance, which is the ratio of the flux linkage λ of the winding $\alpha$to the current i_β that produces the flux. Here, the values of leakage inductance Lls and magnetizing inductance Lm are the same as those of a PMSM. From Eqs. (II.7)(II.9), the stator voltage equation is rewritten as

$$\begin{bmatrix} v_{as} \\ v_{bs} \\ v_{cs} \end{bmatrix} = \begin{bmatrix} R_s & 0 & 0 \\ 0 & R_S & 0 \\ 0 & 0 & R_S \end{bmatrix} \begin{bmatrix} i_{as} \\ i_{bs} \\ i_{cs} \end{bmatrix} + \begin{bmatrix} L_s & M & M \\ M & L_s & M \\ M & M & L_s \end{bmatrix} \frac{d}{dt} \begin{bmatrix} i_{as} \\ i_{bs} \\ i_{cs} \end{bmatrix} + \begin{bmatrix} e_{as} \\ e_{bs} \\ e_{cs} \end{bmatrix} \tag{II. 11}$$

here, since ias 1 ibs 1 ics 5 0, the mid-term of Eq. (II.11) is reduced as

$$\frac{d}{dt}[L_s i_{as} + M i_{bs} + M i_{cs}] = \frac{d}{dt}[L_s i_{as} - M i_{as}] \tag{II. 12}$$

Thus Eq. (II.11) becomes the following voltage equations[22].

$$\begin{bmatrix} v_{as} \\ v_{bs} \\ v_{cs} \end{bmatrix} = \begin{bmatrix} R_s & 0 & 0 \\ 0 & R_s & 0 \\ 0 & 0 & R_s \end{bmatrix} \begin{bmatrix} i_{as} \\ i_{bs} \\ i_{cs} \end{bmatrix} + \begin{bmatrix} L_s - M & 0 & 0 \\ 0 & L_s - M & 0 \\ 0 & 0 & L_s - M \end{bmatrix} \frac{d}{dt} \begin{bmatrix} i_{as} \\ i_{bs} \\ i_{cs} \end{bmatrix} + \begin{bmatrix} e_{as} \\ e_{bs} \\ e_{cs} \end{bmatrix} \quad \text{(II.13)}$$

Voltage Equation of a Brushless Direct Current Motor:

$$v_{as} = R_s i_{as} + (L_s - M)\frac{di_{as}}{dt} + e_{as} \quad \text{(II. 14)}$$

$$v_{bs} = R_s i_{bs} + (L_s - M)\frac{di_{as}}{dt} + e_{bs} \quad \text{(II. 15)}$$

$$v_{cs} = R_s i_{cs} + (L_s - M)\frac{di_{cs}}{dt} + e_{cs} \quad \text{(II. 16)}$$

The electromagnetic torque of three-phase BLDC motor can be described by the following four equations:

$$T_e = \frac{1}{\omega_r}(E_a i_a + E_b i_b + E_c i_c) \quad \text{(II.17)}$$

The generated back-EMF is trapezoidal in shape due to permanent magnet straddling on the rotor and its expression is given below:

$$E_a = K_e * \frac{d}{dt}(\theta) * \omega_r(t) \quad \text{(II.18)}$$

$$E_b = K_e * \frac{d}{dt}\left(\theta - \frac{2\pi}{3}\right) * \omega_r(t) \quad \text{(II.19)}$$

$$E_c = K_e * \frac{d}{dt}\left(\theta + \frac{2\pi}{3}\right) * \omega_r(t) \quad \text{(II.20)}$$

The equation of motion is:

$$\mathbf{J}\frac{\mathbf{d}}{\mathbf{dt}}\boldsymbol{\omega}_\mathbf{m} + \mathbf{B}\boldsymbol{\omega}_\mathbf{m} = \mathbf{T_e} - \mathbf{T_1} \quad \text{(II.21)}$$

II.4 Modeling and simulation of inverter associated to BLDC motor:

The two-level three-phase voltage inverter consists of two switches per arm. The latter have the particularity of being bidirectional and fully controllable when opening and closing. They can be either MOSFETs for low powers and very high frequencies, IGBTs for large powers and high frequencies, or GTOs for very high powers and low frequencies. To ensure the flow of current in both directions, the switch must be placed in antiparallel with a diode.

The general structure of a two-level voltage inverter is shown in Figure.III.3.

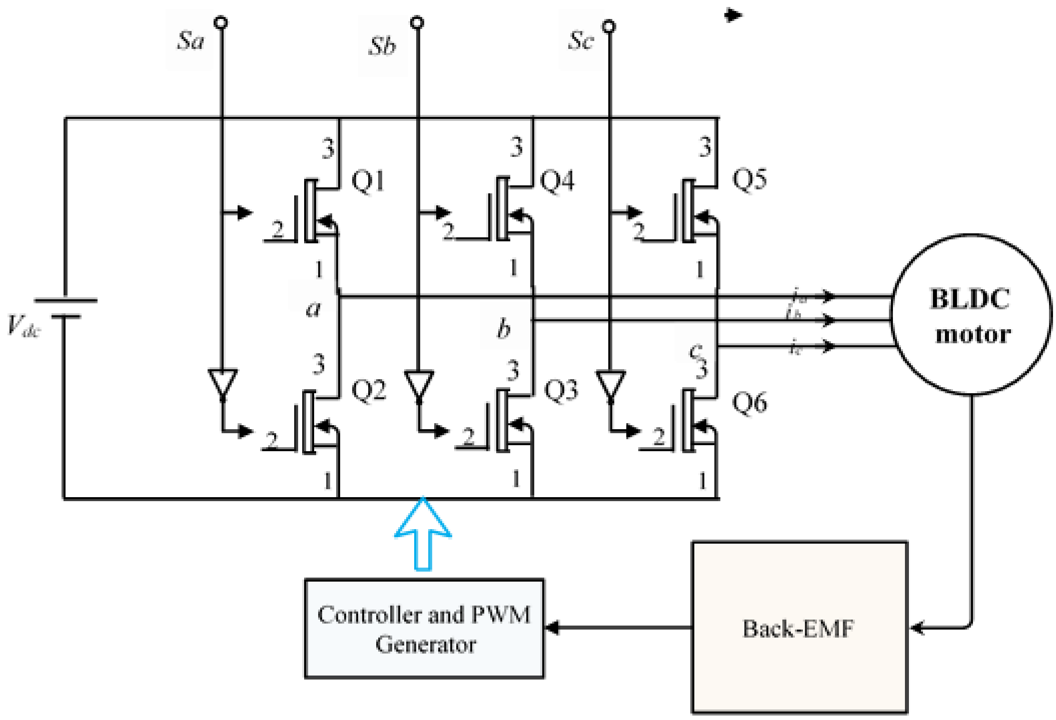

Figure II. 3: Diagramme of a associated BLDC with inverter[20].

The reference voltages are the desired phase-to-neutral voltages Uan, Ubn, Ucn referenced with respect to the neutral point.

The state of the switches, assumed to be perfect, can be defined by three Boolean command quantities Si (i= a, b, c):

- If = 1 the case where the top switch is closed and the bottom one open.
- If = 0 the case where the top switch is open and the bottom one closed.

Under these conditions, the phase voltages Uao, Ubo and Uco can be written as a function of the control signals Si:

$$U_{ao} = \begin{cases} \frac{V_{dc}}{2}, & Sa = 1 \\ -\frac{V_{dc}}{2}, & Sa = 0 \end{cases} \rightarrow U_{ao} = Ka * \frac{V_{dc}}{2} \quad \text{(II.22)}$$

$$U_{bo} = \begin{cases} \frac{V_{dc}}{2}, & Sb = 1 \\ -\frac{V_{dc}}{2}, & Sb = 0 \end{cases} \rightarrow U_{bo} = Kb * \frac{V_{dc}}{2} \quad \text{(II.23)}$$

$$U_{co} = \begin{cases} \frac{V_{dc}}{2}, & Sc = 1 \\ -\frac{V_{dc}}{2}, & Sc = 0 \end{cases} \rightarrow U_{co} = Kc * \frac{V_{dc}}{2} \quad \text{(II.24)}$$

From the definition of the equations Uao, Ubo and Uco, we have Ka, Kb and Kc presents the situation 1 or -1 depends on Si.

The load is considered to be balanced, resulting in:

$$U_{an} + U_{bn} + U_{cn} = 0 \quad \text{(II.25)}$$

$$\begin{cases} U_{ao} + U_{on} = U_{an} \\ U_{bo} + U_{on} = U_{bn} \\ U_{co} + U_{on} = U_{cn} \end{cases} \quad \text{(II.26)}$$

From the sum of equations (II.22), we have

$$(\boldsymbol{U_{ao}} + \boldsymbol{U_{bo}} + \boldsymbol{U_{co}}) + \boldsymbol{3}\ \boldsymbol{U_{on}} = \boldsymbol{U_{an}} + \boldsymbol{U_{bn}} + \boldsymbol{U_{cn}} \tag{II.27}$$

Substituting (4) into (6) gives us:

$$U_{on} = -\frac{1}{3}\ (U_{ao} + U_{bo} + U_{co}) \tag{II.28}$$

Substituting ((II.25)) in ((II.26)) we get:

$$\begin{cases} U_{an} = \frac{2}{3}\ U_{ao} - \frac{1}{3}U_{bo} - \frac{1}{3}U_{co} \\ U_{bn} = -\frac{1}{3}\ U_{ao} + \frac{2}{3}U_{bo} - \frac{1}{3}U_{co} \\ U_{cn} = -\frac{1}{3}\ U_{ao} - \frac{1}{3}U_{bo} + \frac{2}{3}U_{co} \end{cases} \tag{II.29}$$

Substituting (II.22, II.23 and II.24) in (II.29) we obtain:

$$\begin{cases} U_{an} = \frac{2}{3}\ Ka * \frac{V_{dc}}{2} - \frac{1}{3}Kb * \frac{V_{dc}}{2} - \frac{1}{3}Kc * \frac{V_{dc}}{2} \\ U_{bn} = -\frac{1}{3}Ka * \frac{V_{dc}}{2} + \frac{2}{3}Kb * \frac{V_{dc}}{2} - \frac{1}{3}Kc * \frac{V_{dc}}{2} \\ U_{cn} = -\frac{1}{3}Ka * \frac{V_{dc}}{2} - \frac{1}{3}Kb * \frac{V_{dc}}{2} + \frac{2}{3}Kc * \frac{V_{dc}}{2} \end{cases} \tag{II.30}$$

The different combinations of the three quantities (Ka, Kb, Kc) make it possible to generate eight voltage vectors, two of which correspond to the zero vector. With the phase-to-neutral voltages as a function of the command quantities:

$$\begin{bmatrix} U_{an} \\ U_{bn} \\ U_{cn} \end{bmatrix} = \frac{V_{dc}}{2} \begin{bmatrix} \frac{2}{3} & -\frac{1}{3} & -\frac{1}{3} \\ -\frac{1}{3} & \frac{2}{3} & -\frac{1}{3} \\ -\frac{1}{3} & -\frac{1}{3} & \frac{2}{3} \end{bmatrix} \begin{bmatrix} Ka \\ Kb \\ Kc \end{bmatrix} \tag{II.31}$$

Thus, the model presented in equation 31 expresses the three-phase inverter.

II.4.1 Simulation results and discussion:

The design of BLDC motor is verified using parameters listed in Table 1 and modeled in MATLAB SIMULINK environment to verify design analysis of Brushless DC motor. A Faulhaber BLDC motor and Motor driver rated current 10A peak have been taken for simulation with BLDC motor is set value of 10000rpm speed and simulated performance of motor at no load and loaded condition is presented MATLAB based on transfer function, state space modeling as shown in Figure II.5 and transfer equations in open-loop condition and results is presented in Figure II.9 [23].

Table II. 1: Test for idenfuction of indectence BLDC motor

V	**0.114**	**O.204**	**0.26**	**0.32**	**0.35**	**0.39**	**0.42**	**0.48**
I	**0.5**	**1**	**1.3**	**1.6**	**1.8**	**2**	**2.2**	**2.5**
X	**0.228**	**0.204**	**0.2**	**0.2**	**0.194**	**0.195**	**0.190**	**0.192**
L	**0.000726**	**0.000649**	**0.00636**	**0.000636**	**0.000618**	**0.000621**	**0.000605**	**0.000611**

Table II. 2: BLDC Motor parameters[7]

Motor Data A2212/13T	
Kv	**1000RPM/V**
Max Efficiency	**80%**
Max Efficiency current	**4-10A(>75%)**
No load current	**0.5A@ 10V**
Resistance	**0.090 ohms**
Max current	**13A for 60S**
Max Watts	**150W**
Weight	**52.7 g /1.86 oz**
Size	**28mm dia x 28 mm bell length**
Shaft Diameter	**3.2 mm**
Poles	**14**
Model Weight	**300-800g/10.5-28.2 oz**
No. Of Cells	**2-3Li – Poly** **6-10 Ni Cd/NiMH**

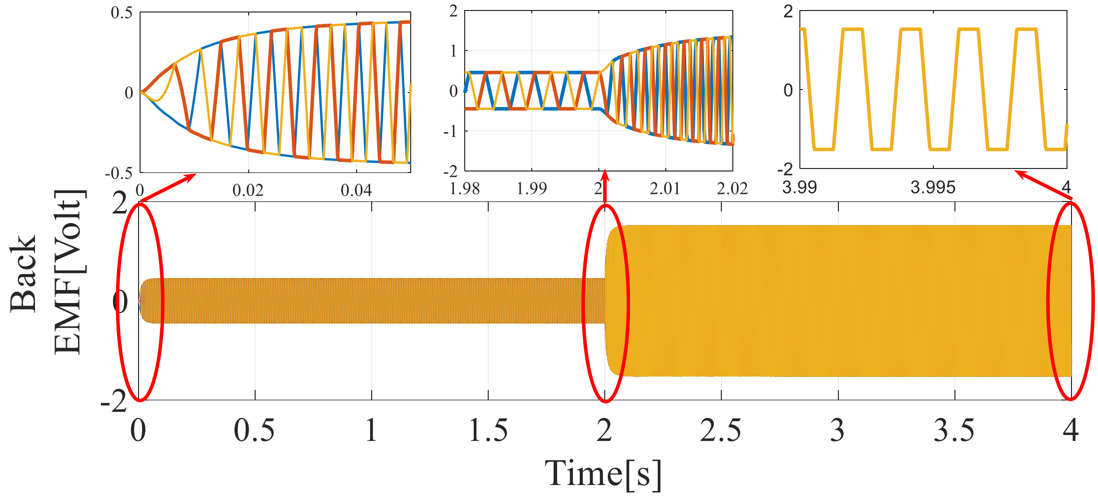

Figure II. 4: Back EMF generated for Phase A, Phase B and Phase C for BLDC with inverter.

The figure II.4, shows the back EMF created by three phases for BLDC with inverter, at instant 2s, back-EMF increases according to the increase in the reference voltage.

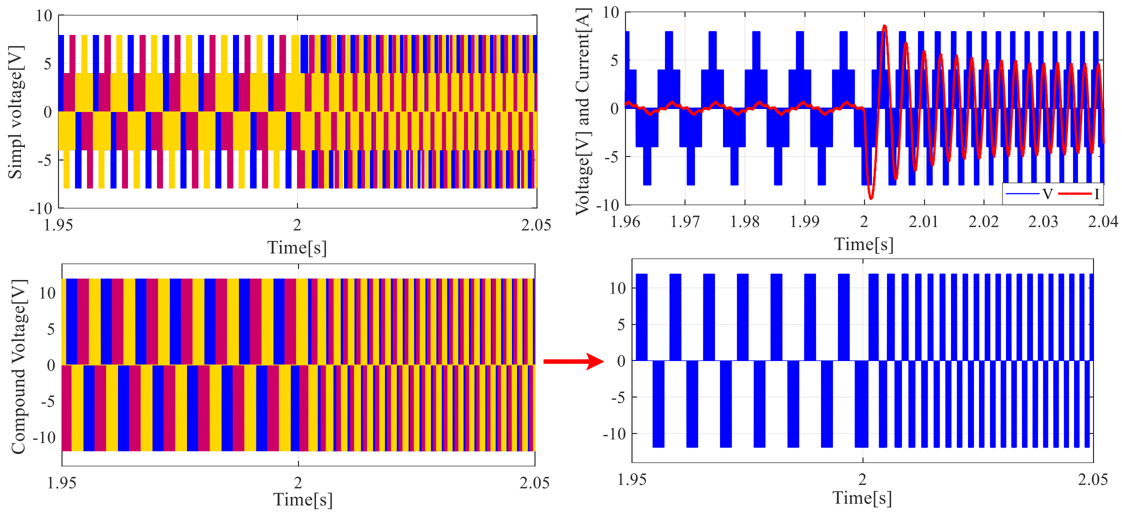

Figure II. 5: Voltage and current as a function of time of BLDC with inverter.

The figure II.5, represents evaluation voltage and current, after the instant 2s, the value of the voltage increases with the increase of the value of the current in one phase where the voltage grows in accordance with the reference input, as the reference increases.

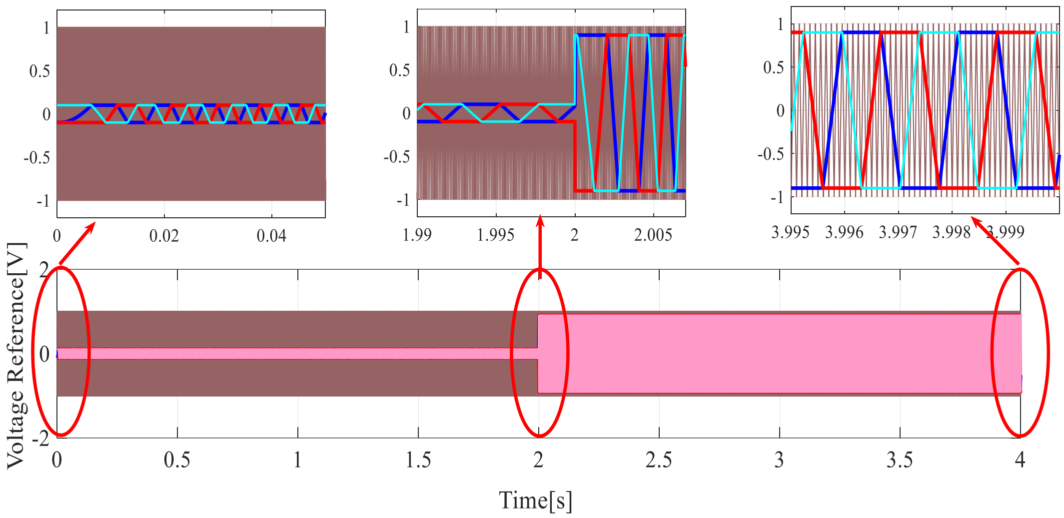

Figure II. 6:. Evolution reference voltage as a function of time for BLDC with inverter.

The figure II.6, represents evolution reference voltage as a function of time for BLDC with inverter, at instant 2s, the voltage increases depending on the results we want to get.

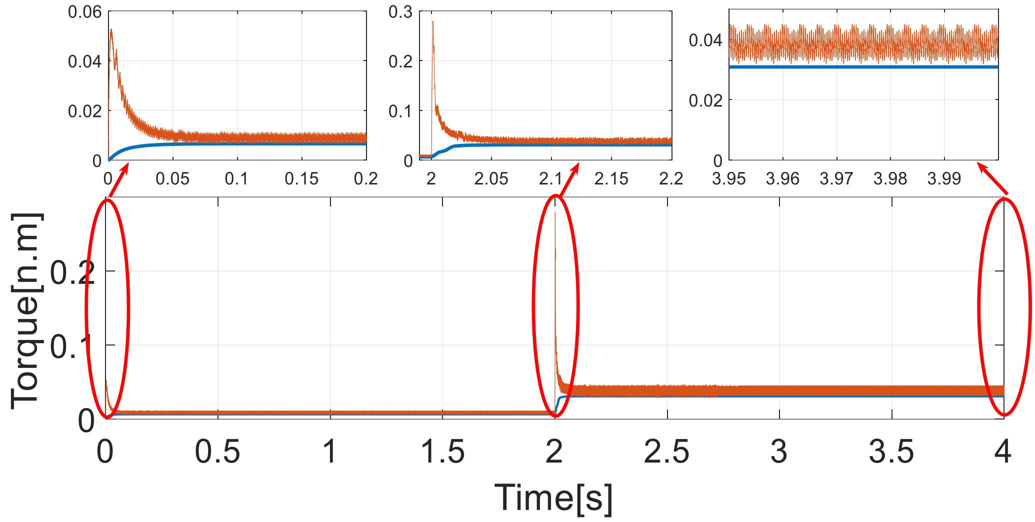

Figure II. 7: Electromagnetic torque with load torque for the BLDC with inverter.

The figure II.7, shows the electromagnetic torque with the load torque, where we note that the compatibility between the two torques with torque load disturbances because the inertia torque is very low.

II.5 Speed control by PI regulator:

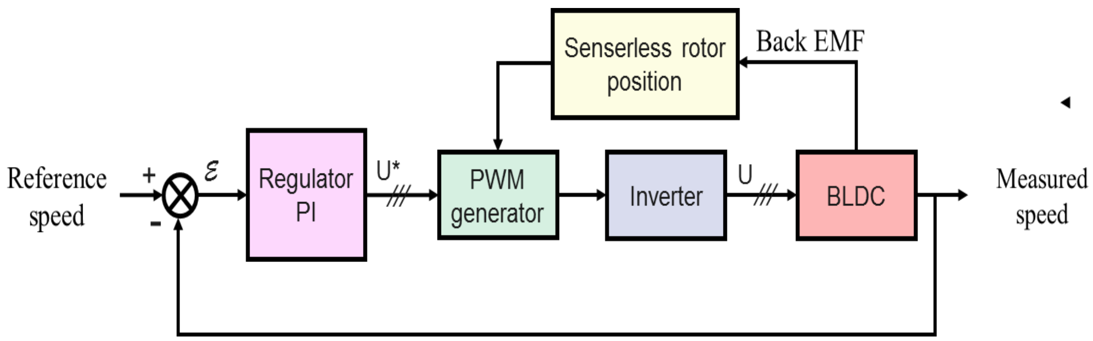

Figure II. 8: Diagram of closed loop speed control system of BLDC motor associated with inverter.

Figure II.8, depicts the most basic speed control method for controlling the speed of a BLDC motor. For speed control, a proportional integral (PI) is typically utilized. The motor voltage reference (or PWM duty) is output by this PI speed controller.

$$U^* = \left(Kp + \frac{Ki}{S}\right) \cdot (W_m^* - W_m) \qquad K_P = 0.015 \quad K_i = 0.03 \qquad \text{(II.32)}$$

Where Kp and Ki are the PI speed controller's proportional and integral gains, respectively.

This reference voltage is generated using a PWM method for inverter then applied to the BLDC motor to obtain a better dynamic response of the speed control, the system compare the measured speed from optical sensor and reference speed to obtain the error, the latter going through PWM generator to obtain reference voltage from the rotor position by using the sensor less technique by Back EMF. When, the voltage reference produced and compared to sequence repeating in order to obtain the PWM exploited to the inverter for determining the voltage (Va, Vb, Vc).

The BLDC motor generates a mechanical power that presented in speed and torque after supplied and controlled the inverter [24].

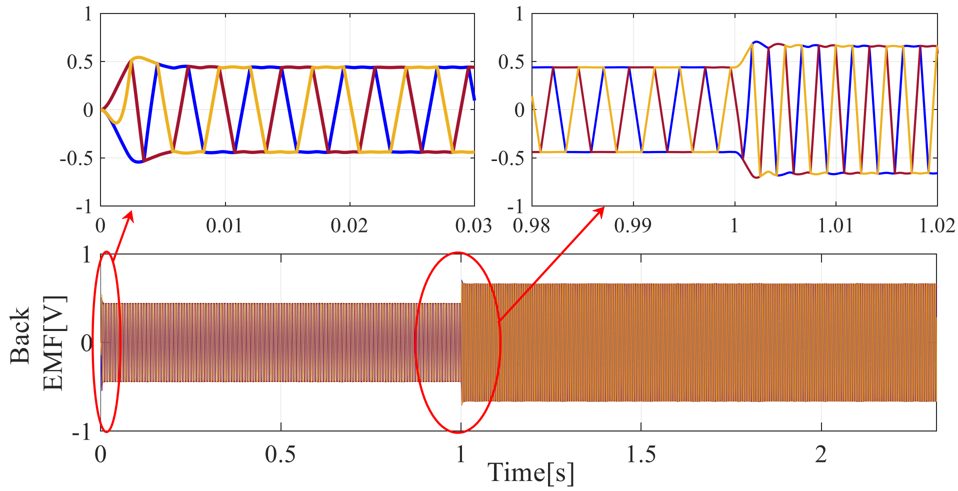

Figure II. 9: Back EMF generated for Phase (a, b, c) as a function of time for speed control system.

The figure II.9, shows the back EMF created by three phases BLDC for speed control system, at the instant 1s the EMF value increases instantaneously in proportion to the reference input, when the speed reference is increases, the RMS voltage and the current also increase, the worth rises from here.

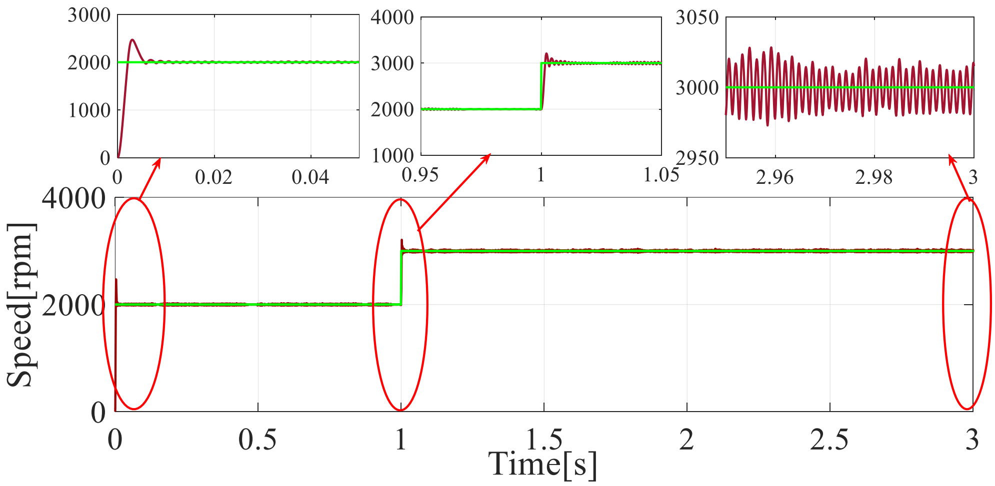

Figure II. 10: Evaluation reference and measured speed for the control system.

The figure II.10, represents the comparison between the measured and the reference speed, where we notice compatibility between the two speeds with the presence of disturbances in the measured speed because the inertia torque is very low.

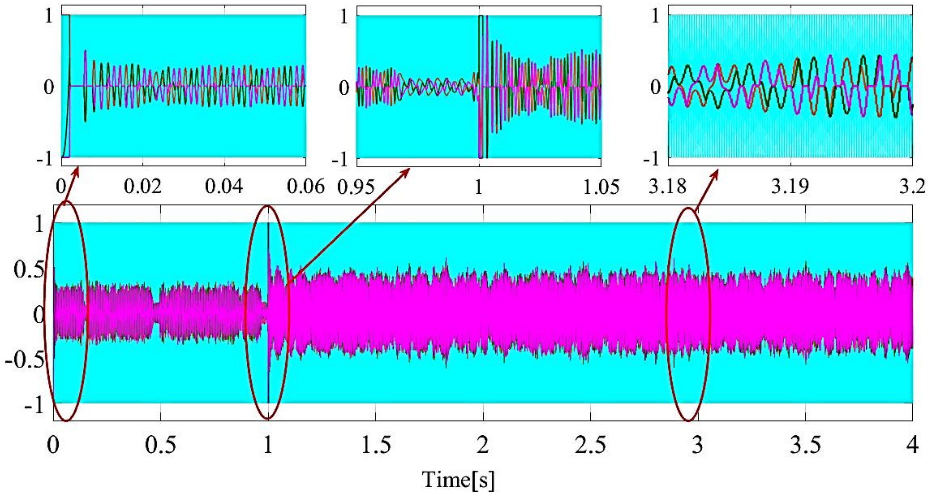

Figure II. 11: PWM control as a function of time for speed control system.

The figure II.11, represents the reference voltage, between the instant 0 at 1 s, with the rise in value after 1 that when the speed reference is increases, This means that torque is not enough.

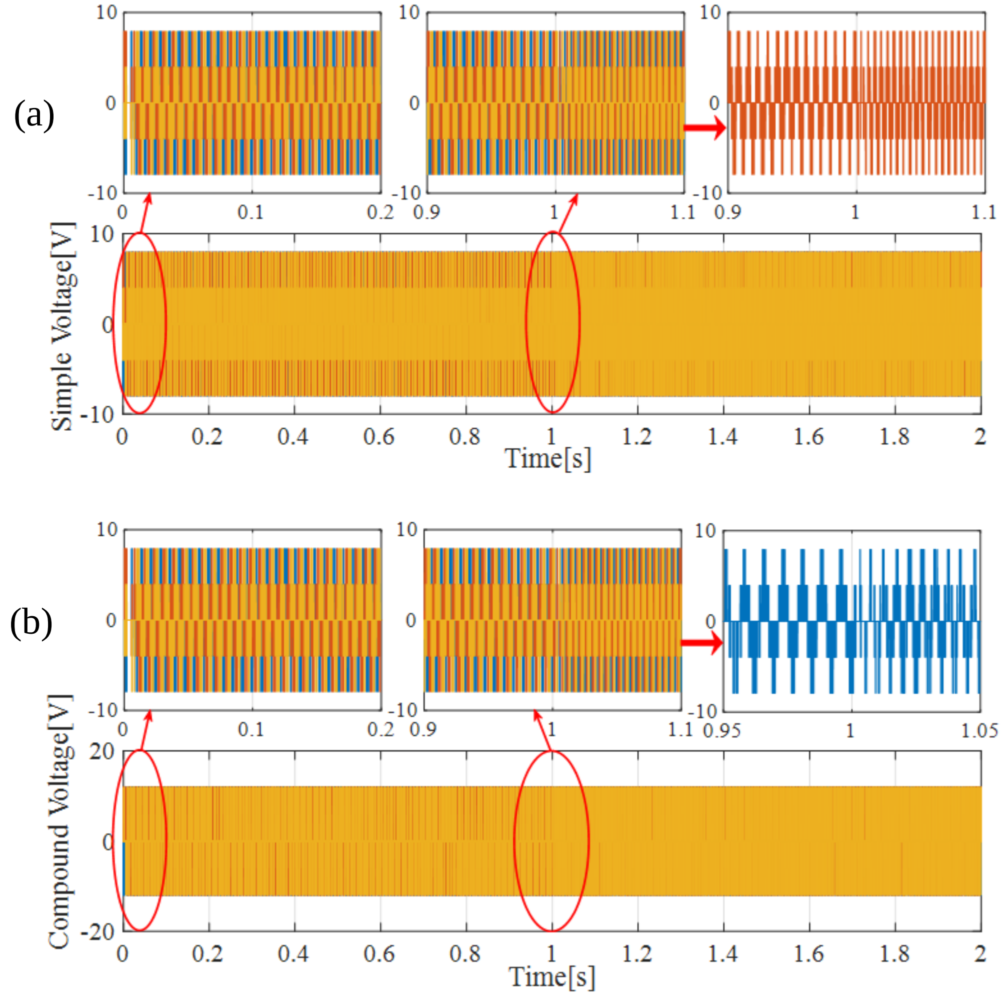

Figure II. 12: (a) Evaluation simple voltage, (b) Evoluation compound as a function of time for speed control system**.**

Figure II.12, represents evaluation simple and compound voltage as a function of time for speed control system, at instant 1s, the voltage grows in accordance as the reference value increases (the voltage increases according to the motor speed).

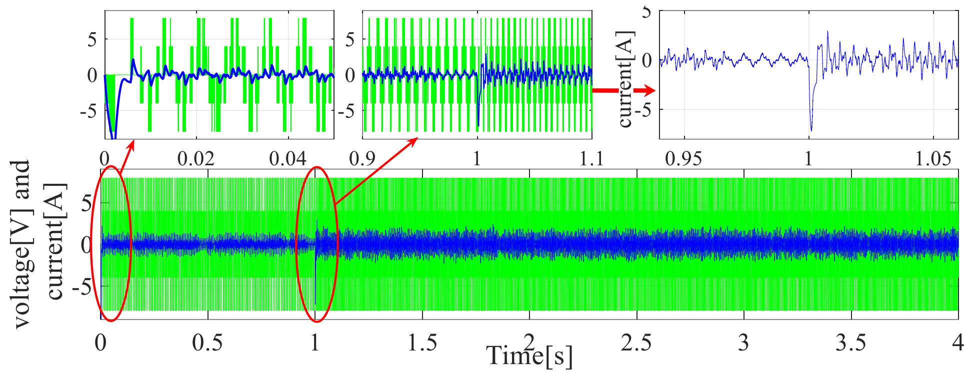

Figure II .13.: voltage and current as a function of time for speed control system.

The figure II.13, represents the voltage and current as a function of time for speed control system, an increase in voltage correlates to an increase in current, according to the reference speed.

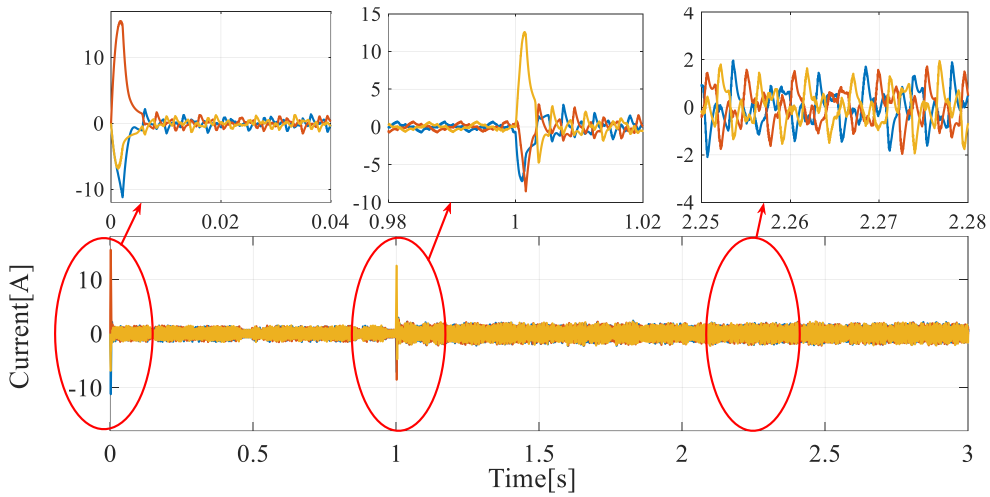

Figure II. 14: The output current (a, b, c) of inverter associated with BLDC for speed control system.

The figure II.14, displays the current of three-phase as a function of time for speed control system, at the instant 1s, the current grows in proportion to the reference input, as the reference increases, the period decreases in proportion to the motor speed.

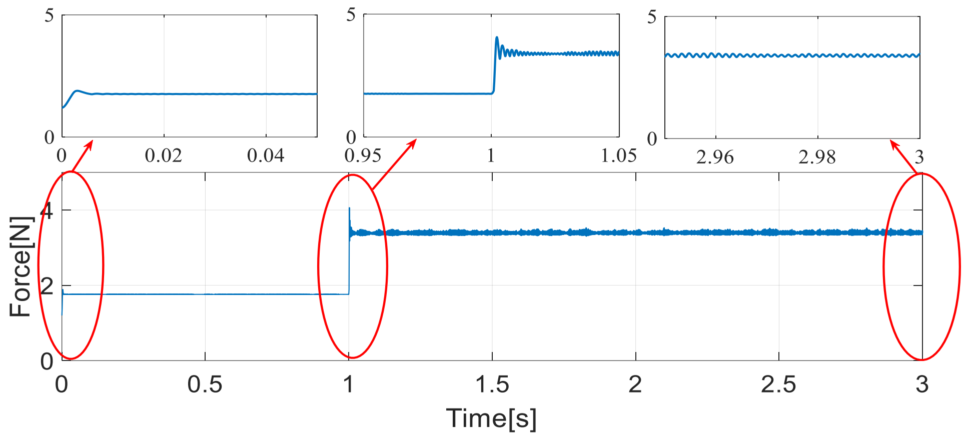

Figure II. 15: Evaluation of the force as a function of time for the speed control system.

The figure II.15, represents the force, at moments 0 and 1s, the force increases Instant increase, and at instant 1s the force increases according to the reference input when the reference increases.

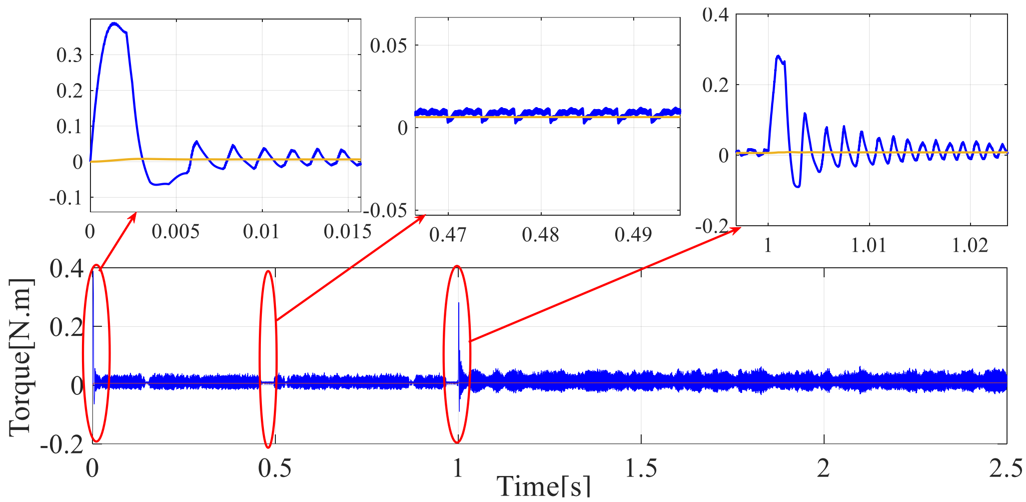

Figure II. 16: Electromagnetic torque with load torque for the control system.

The figure II.16, shows the electromagnetic torque with load torque, where we notice compatibility between the two torques with the existence of disturbances in the load torque, because the inertia torque is very low.

II.6 Conclusion:

Quad-copter with an accelerating industry is an interesting platform to perform different control strategies. The mathematical model of BLDC with inverter was developed and implemented in Simulink for it will be ready to implementation on the real hardware to control of one axe of drone. The structure was built successfully using the selected components, compatible with each other. The structure Simulink model was made, based on derived differential equations of motion. A PI-based controller was designed and tuned for speed control based on reference voltage. The results of proposed strategy confirm the effectiveness of proposed control for applied in real time in next chapter.

Chapter III: Experimental data for real time dynamic control of BLDC motor with mechanical system

III.1 Introduction

The choice of materials is an important step in the realization of a drone to guarantee a light and solid structure capable of withstanding a difficult landing.

In this chapter, we will identify the data parameter of the BLDC motor and the mechanical system validation model by experimental data. Where we will in the last part, the reel time speed control and angle control for stabilization of the mechanic system represent some part in studies Quadra-copter. In order to achieve the result present, the effectiveness of proposed dynamic control of BLDC motor with the mechanical system.

III.2 Identification parameters

The diagram for accusation data of model BLDC with mechanical system by controlling and revises the reference voltage. In order to extracting the data we use gyroscope sensor, speed sensor, voltmeter, end ampere meter. Otherwise, the object for dynamic control in the speed control and angle control stabilization.

We also select the data of speed sensor and gyroscope sensor, otherwise with PWM control, the switches of the inverter are controlled based on a comparison of a sinusoidal control signal and a triangular switching signal. Hence, the BLDC motor is start according the reference voltage then the mechanical system that connect of propeller and the weight of accessorize (motor, controller, sensor….) the scale gives the weight of system. The gyroscope sensor send information controller and we take the DATA angle from PC. Also, the speed sensor gives information to PC by communication serial the take a DATA for each reference voltage.

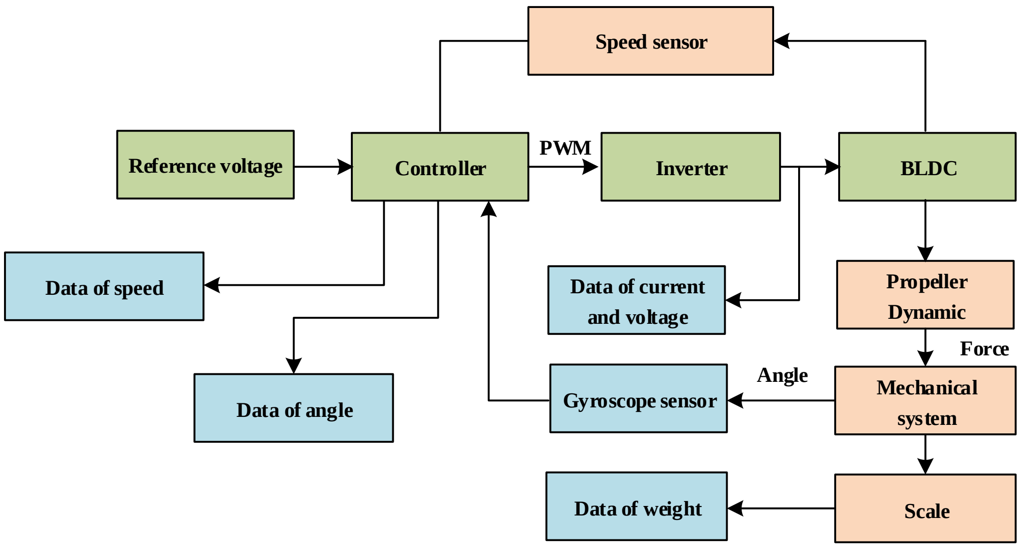

Figure III. 1: Diagram of acusition DATA of indentufication BLDC,Inverter and mechnical system.

III.3 Exprimental data of BLDC and mechanical system

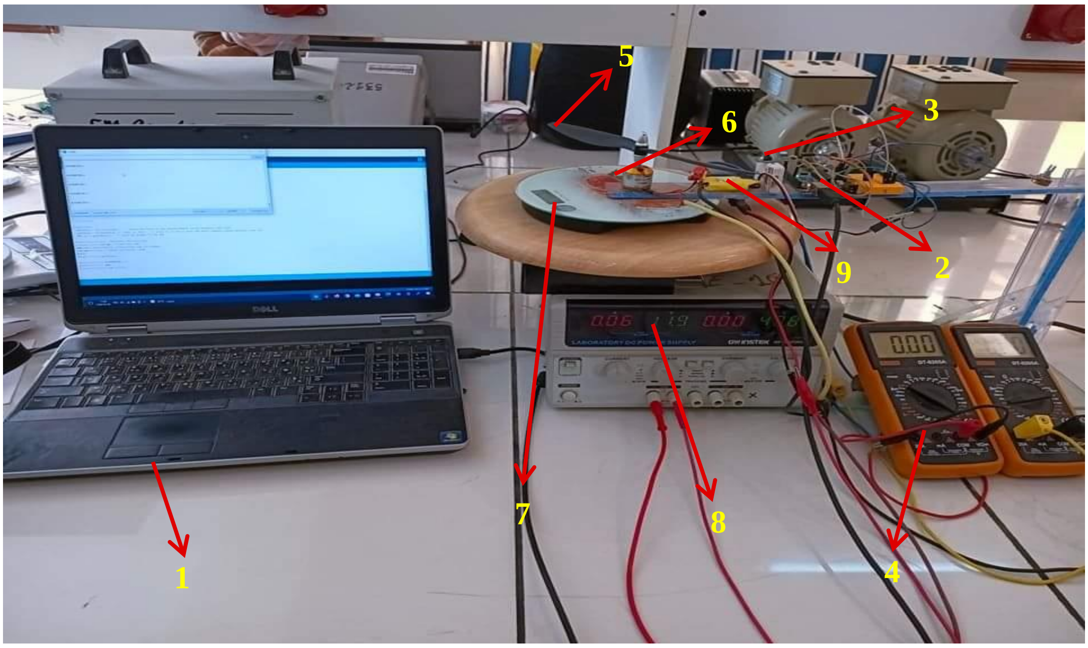

Figure III. 2: Test bench for data acquisition of speed, weight, electrical and mechanical power of BLDC motor and mechanical system.

Equipment and tools used to Exprimental data:

1- PC
2- Arduino
3- Speed sensor
4- Multimeter device
5- Probller
6- BLDC Motors
7- Scale
8- Alimentation
9- Inverter

The time rotor parameters were measured only by self-loading weighing 214 grams. Overall, the results are shown in Table III.1. It can be seen that when the speed increase the force increases also.

Table III. 1: Identification of data parameters for speed, weight, electrical and mechanical power of BLDC motor and mechanical system.

Vref%	3	9	14	23	31	39	44	50	57	60	70
***Speed*(RPM)**	2500	3000	3500	4000	4500	5000	5500	6000	6500	7000	7500
V_{RMS}(V)	3.10	3.40	4.26	4.62	4.75	4.68	4.86	5.27	5.58	5.70	6.25
I_{RMS}(A)	0.45	0.55	0.90	1.15	1.55	1.80	2.13	3.10	3.20	3.45	3.84
M(kg)	0.012	0.019	0.034	0.05	0.069	0.084	0.105	0.148	0.202	0.214	0.250
***F*(N)**	0.12	0.19	0.34	0.5	0.69	0.84	1.05	1.48	2.02	2.14	2.5

V_{dc}(V)	11.9	11.9	11.9	11.9	11.9	11.9	11.9	11.9	11.9	11.9	11.9
I_{dc}(A)	0.22	0.26	0.42	0.54	0.77	0.97	1.22	1.91	2.12	2.42	3.01
P_{in}(W)	2.618	3.094	4.998	6.426	9.163	11.543	14.518	22.729	25.228	28.790	35.819
P_u(W)	2.09	2.475	3.998	5.14	7.33	9.234	11.614	18.183	20.182	23.032	28.655
T_L(N.m)	0.008	0.009	0.01	0.012	0.156	0.017	0.020	0.028	0.0296	0.0314	0.036

The expression of the input power from DC source can be write as:

$$P_{in} = V_{dc} \times I_{dc} \quad \text{(III.1)}$$

From the efficiency of BLDC motor from data sheet can be calculate the out mechanical power as follow:

$$P_u = P_{in} \times \mu \quad \text{(III.2)}$$

III.4 Mechanical model:

The hardware setup includes a light rod connected to a plastic stand through a low friction potentiometer, the opposite give-up of the rod has a BLDC motor driving a 25.4 cm propeller output voltage of the potentiometer is discrete using and virtual converter and is sent to MATLAB right here USB protocol MATLAB routinely adjusts the offset within the sign via subtracting the preliminary fee and multiplies it with the predetermined advantage to transform the voltage into an angular studying.

The favored manage signal is then fed back to the version the use of a pulse width modulation an h-bridge circuit is used to permit directional operation, that is high quality manage sign drives the propeller within the ahead Direction, poor control signal drives it in the reverse path, that is the arrow pendulum design constructed on the University of Arizona advanced Microsystems laboratory, the remainder of this presentation might be approximately the design evaluation and implementation of this mechatronics machine the arrow pendulum rotates on a small low friction potentiometer that lets in the microcontroller to encode the attitude of the pendulum at any given time the arrow pendulums rod is fabricated from carbon fiber and includes a small DC micro motor on the unfastened cease, this BLDC micro motor is capable of spinning the connected propeller over 8,000 radians in line with 2nd.

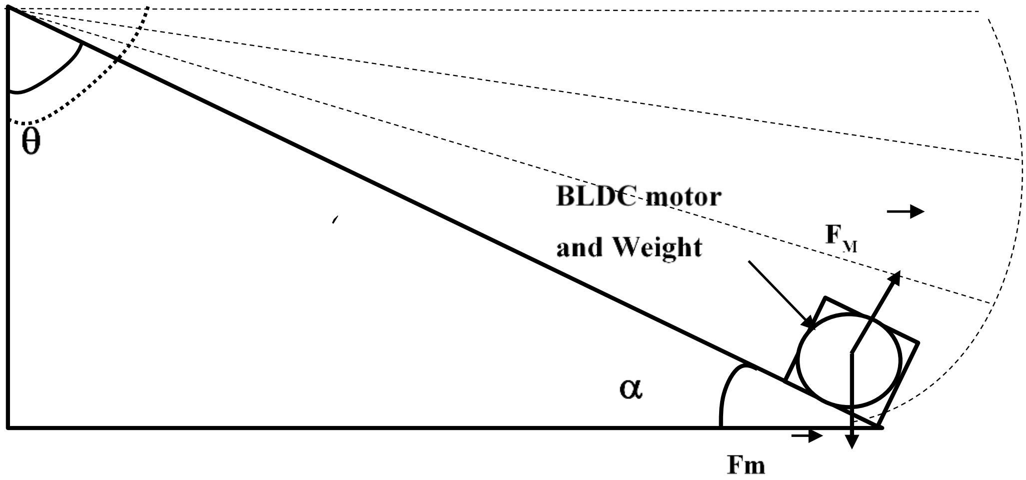

Figure III. 3: micanical system for one axe of studied quadcopter

From Newton's law:

$$\sum T = J\frac{d\omega}{dt} \Longrightarrow T_{Motor} - T_m = J\frac{d\omega}{dt} \quad \text{(III.3)}$$

Where represents:

T: Torque

J: inertie torque

$$T_m = m.g.L\cos\alpha \quad \text{(III.4)}$$

$$T_M = F_M.L \quad \text{(III.5)}$$

In order to develop a mathematical model of the system we substitute the equation (III.4) into Equation (III.3):

$$T_m = mgL\cos(\alpha) \quad \text{(III.6)}$$

We have:

$$\alpha = \frac{\pi}{2} - \theta \quad \text{(III.7)}$$

So:

$$T_m = mgL\cos\left(\frac{\pi}{2} - \theta\right) \quad \text{(III.8)}$$

When we plug Equation (III.5) and (III.9) into Equation (III.3), we get:

$$\boldsymbol{\sum T = J\frac{d\omega}{dt} \Longrightarrow T_{Motor} - T_m = F_M.L - mgL\cos\left(\frac{\pi}{2} - \theta\right) = J\frac{d\omega}{dt}} \quad \text{(III.9)}$$

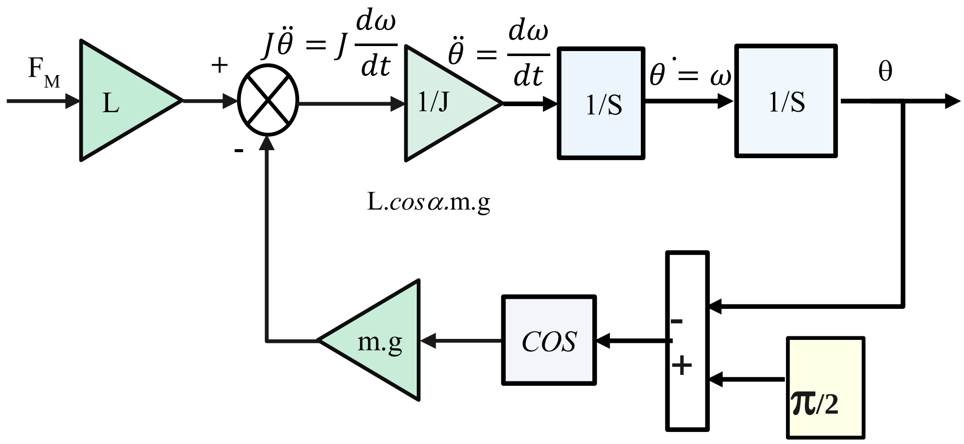

Figure III. 4: Functinal diagram for mechanical model for the studied system.

III.5 Simulation based on experimental data

III.5.1 Speed control based on experimental data

Data acquisition from the previous part used in MATLAB/Simulink for BLDC model. The using data from the experimental test the result more truth that we used in the previous chapter. Through this simulation, we can determine the k_p and k_i for exploited in real time speed control. Hence, the characteristic speed is related to the voltage reference present in figure (III.5). The characteristic force as a function of the voltage reference is present in figure (III.9)

The diagram presented the speed control based on experimental data by PI regulator , for control speed the measured speed compare with the reference speed and regulator PI determine the voltage reference from the last error of speed ,the model data of speed BLDC motor as a function of voltage reference gives the desired an speed.

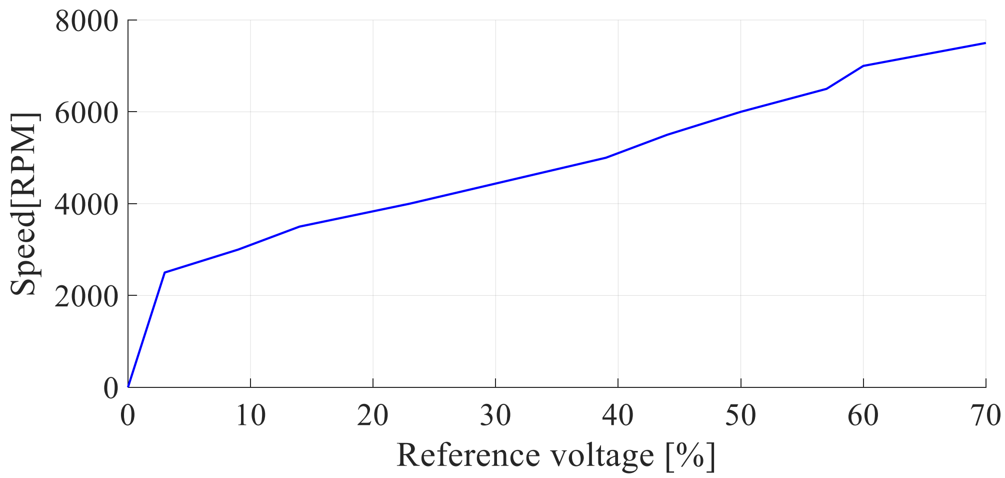

Figure III. 5: Data of BLDC model based on speed as a function of reference voltage from experimental test.

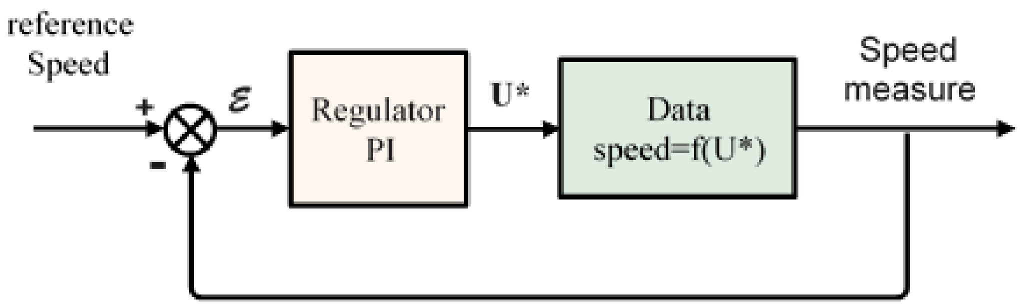

Figure III. 6: Diagram of Speed control based on experimental data.

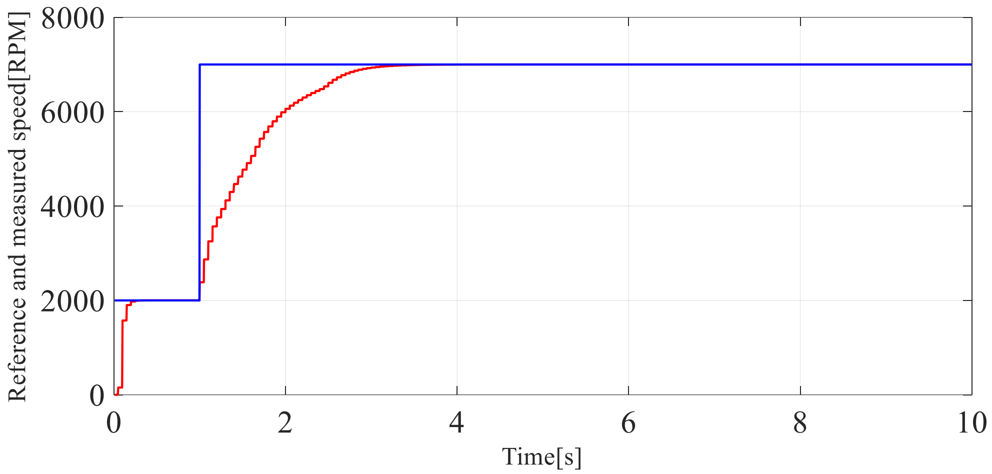

Figure III. 7: Evaluation reference and measured speed as a function of time for speed control based on experimental data.

The figure III.7 represents comparison between reference and measured speed for speed control based on experimental data, from the instant 0s, the measured speed immediately increases to match the reference speed, and it steadily increases, also after the instance 1s the reference speed rise to 7000rpm.

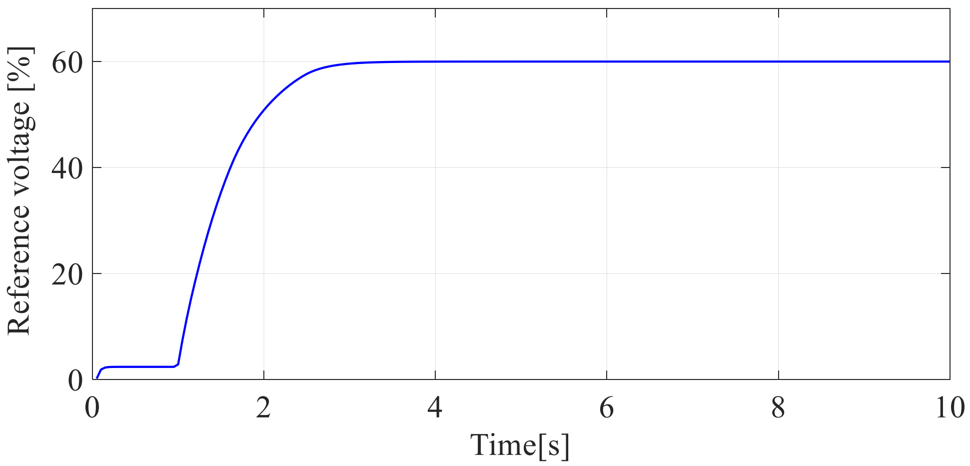

Figure III. 8: Evaluation reference voltage as a function of time for speed control based on experimental data.

The figure III.8 represents evaluation reference voltage for speed control based on experimental data, after instant 1, the voltage percentage gradually increases with increasing motor speed.

III.5. 2 Angel control based on experimental data

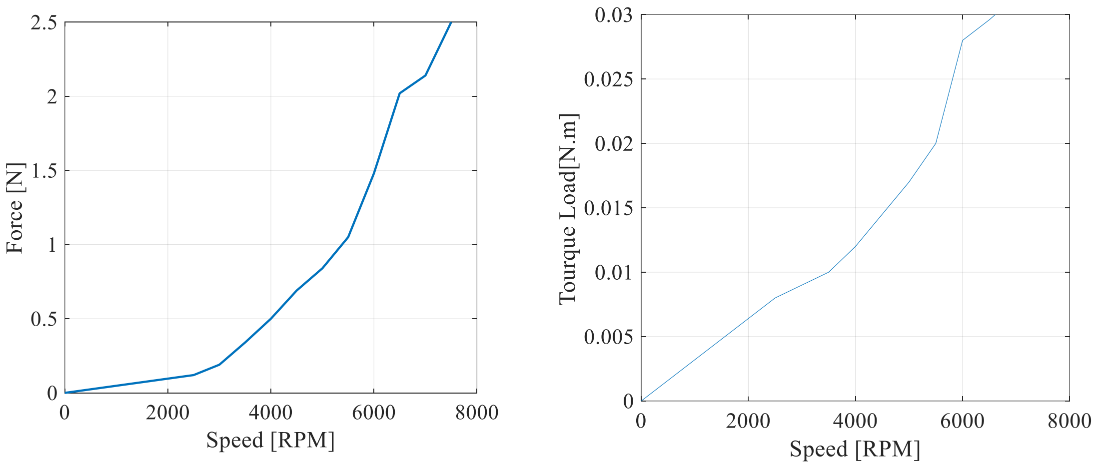

(a) (b)

Figure III. 9: (a) Data parameter of torque load as a function of speed ,(b) Data parameter of force as a function of speed.

Data acquisition from the previous part that we use in MATLAB/Simulation the using data from the experimental text the result more truth that we used in the previous chapter. Hence, the characteristic angle is related to the reference angle present in figure (III.10). The characteristic force as a function of the reference angle is present in figure III.10 the diagram presented the angle control based on experimental data by PI regulator.

For angle control the measured angle compare to the angle reference and the regulator PI determine the voltage reference from the last error of angle, the model data of speed as function of voltage gives the desired angle.

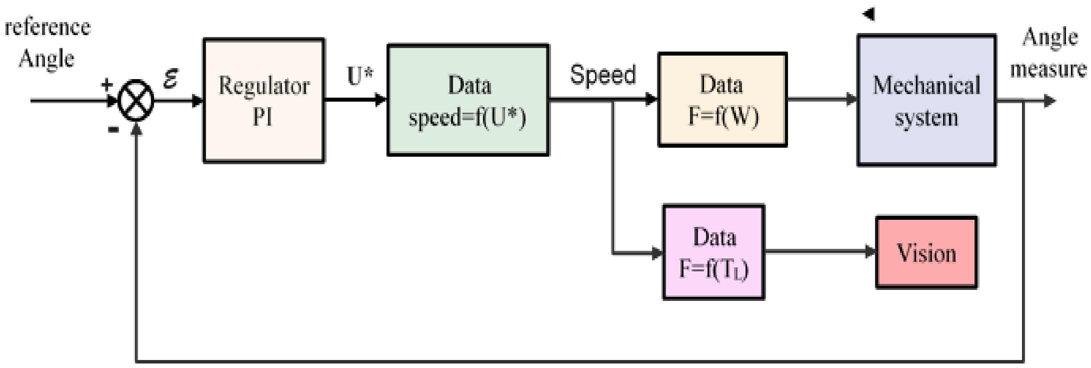

Figure III. 10: Diagram of Diagram of angle control based on experimental data**.**

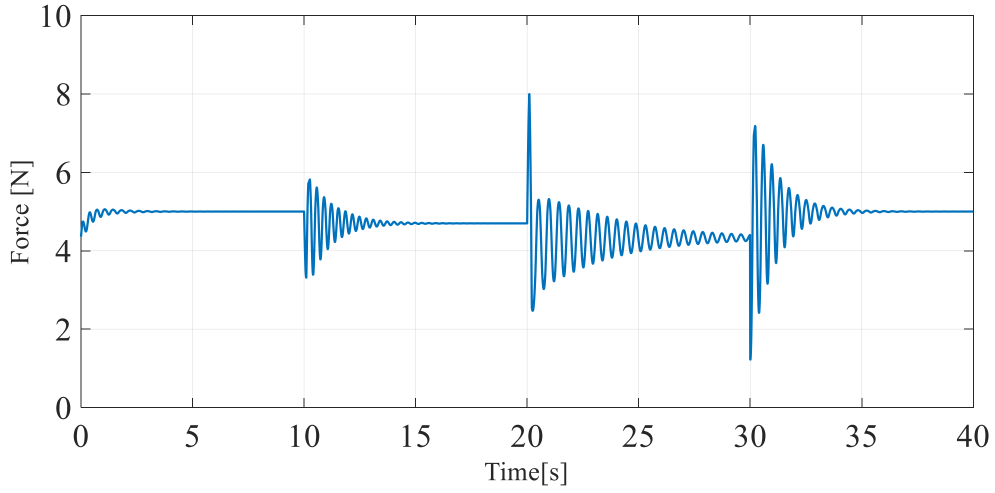

Figure III. 11: Evaluation force as a function of time for angle control based on experimental data.

Figure III.11 represent evolution force as a function of time for angle control based on experimental data, we notice a fluctuation in the force value when the speed increased, which increased due to an increase in the reference voltage.

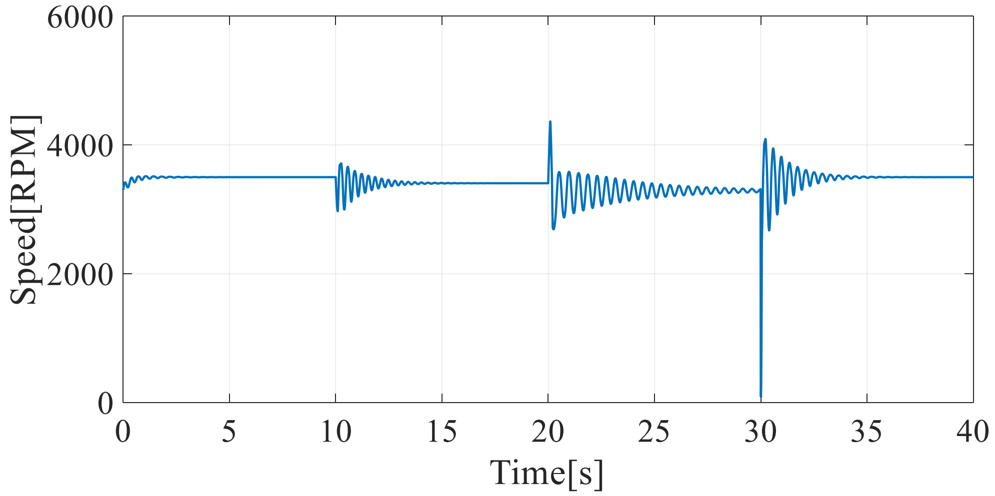

Figure III. 12: Evolution speed as a function of time for angle control based on experimental data.

Figure III.12 represent evolution speed as a function of time for angle control based on experimental data, we notice a fluctuation in the speed value when the reference voltage percentage increased.

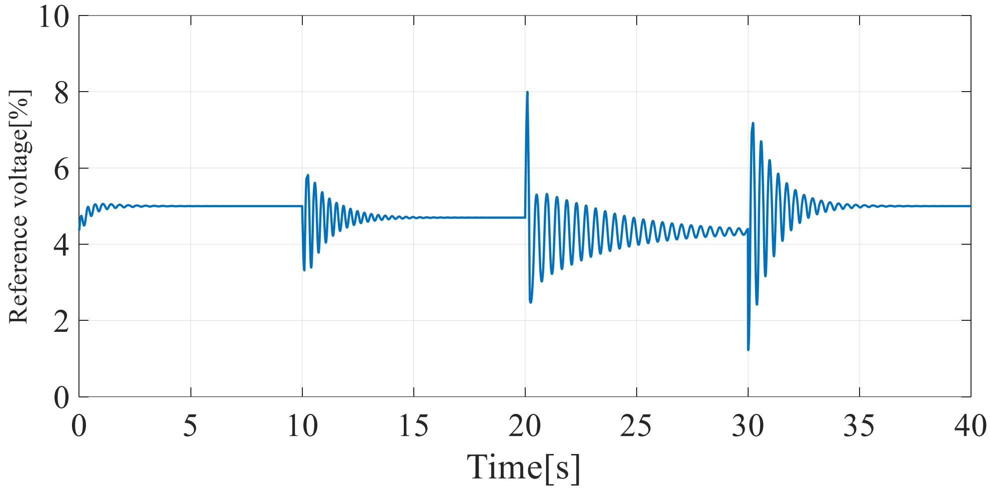

Figure III. 13: Evolution reference voltage as a function of time for angle control based on experimental data.

The figure III.13 represents the evolution of the reference voltage as a function of time, where we control the increase or decrease of the reference voltage according to the results that we want to get.

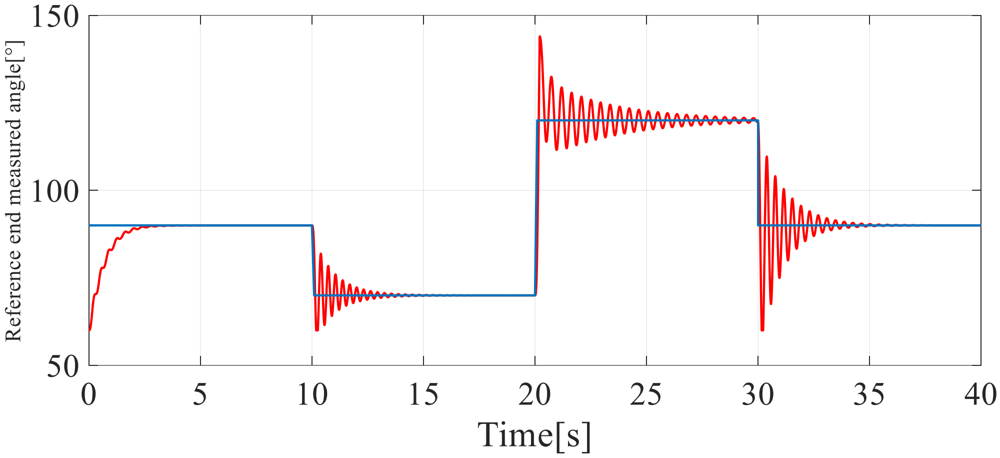

Figure III. 14: Evaluation reference and measured angles for the angle control based on experimental data.

The figure III.14 represent the comparison between the reference and measured angle, where we notice a compatibility between the two angles with the presence of disturbances in the measured speed and this is due of inertia torque is very low.

III.6 Real time experimental of dynamic control

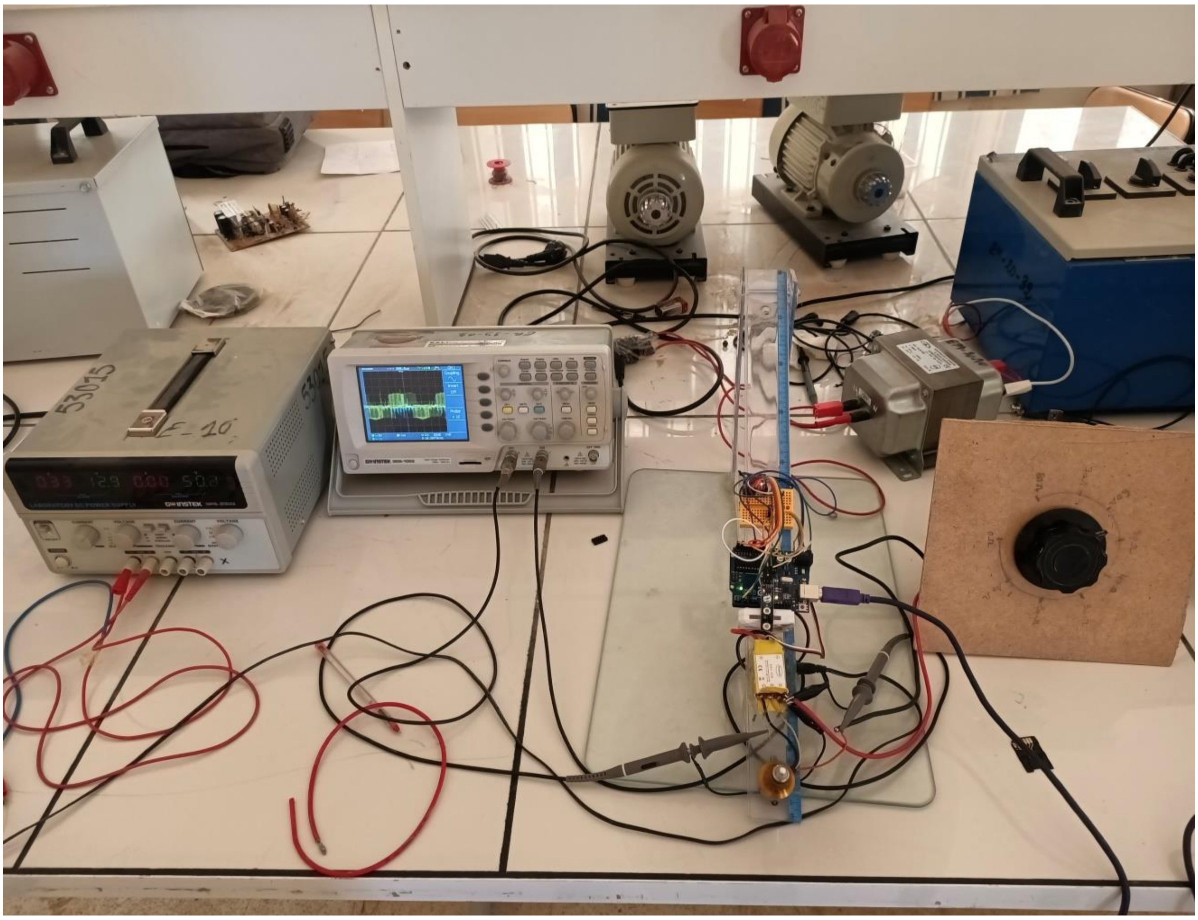

Figure III. 15: Test bench for real time speed and angle control.

- **Closed loop speed control**

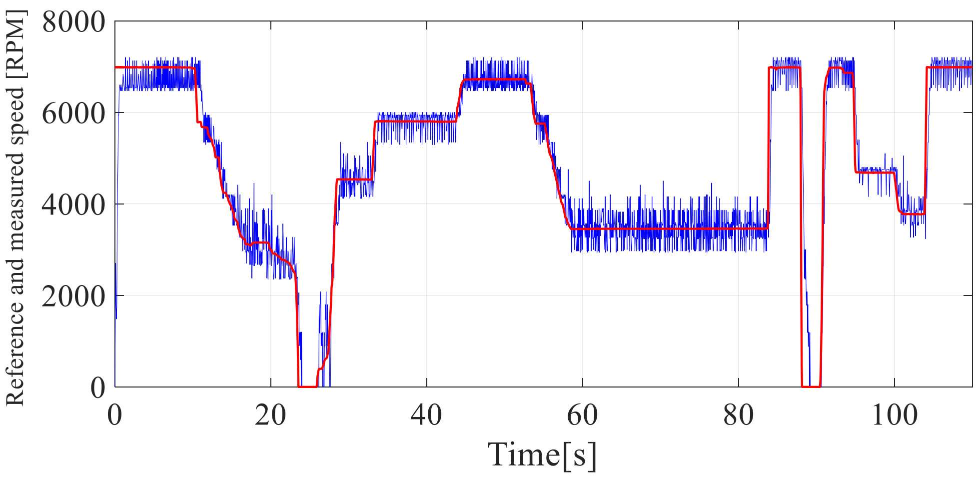

Figure III. 16: Real time speed control of BLDC with inverter**.**

Figure III.16 represent the real time for speed control BLDC with inverter .The reference and measured speed as a function time, we see agreement between the two speeds despite an oscillation in the measured speed, caused by the low inertia torque.

• Closed loop angle control

The angle control for dynamic stabilisation we have the gyroscope sensor gives the angle of mechanical system and compared by the reference angle in the controller by the regulator PI. The reference voltage applied to inverter as PWM signal then the propeller turned for give the force to change the angle of system. In this controller we use speed sensor for granted the take-off motor also for limited speed.

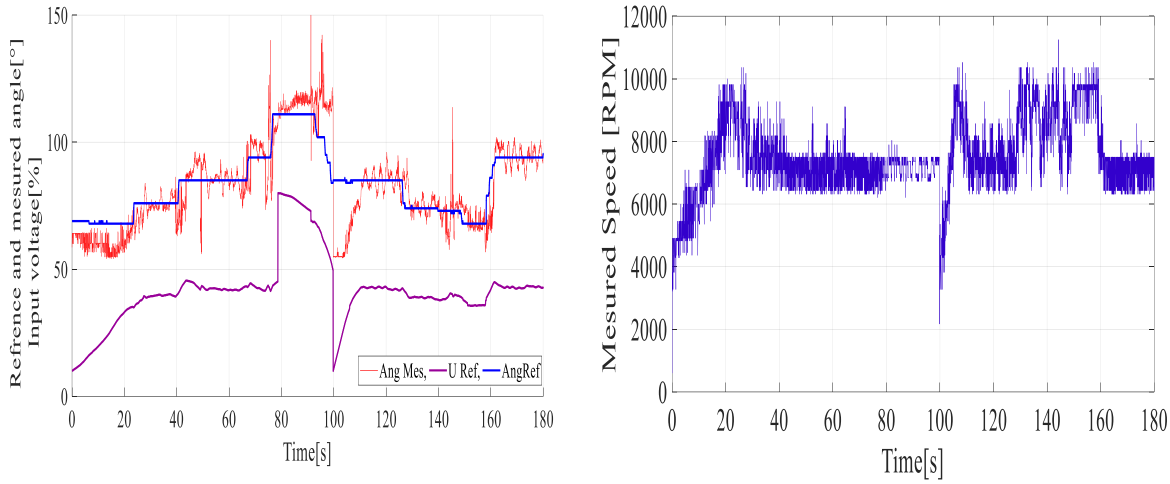

Figure III. 17: Measured speed and reference of angle in a 0.007and 0.003**.**

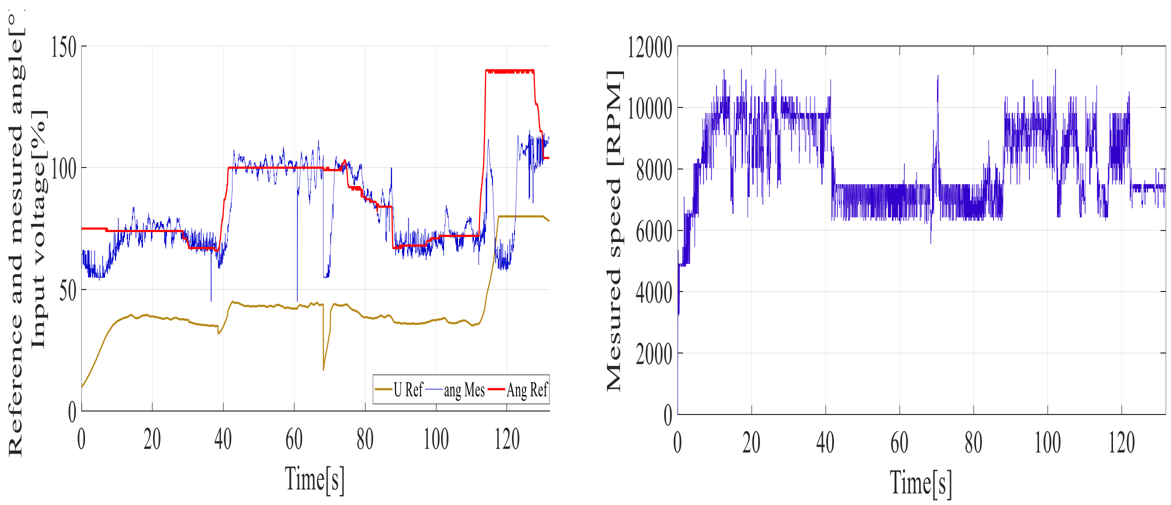

Figure III. 18: Measured speed and reference of angle in a 0.009 and 0.005.

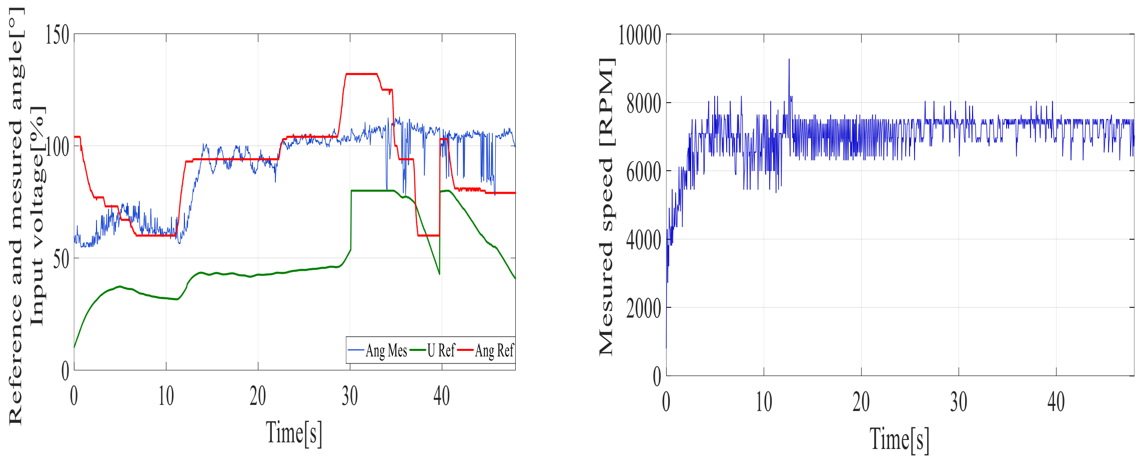

Figure III. 19: Measured speed and reference of angle in a 0.013 and 0.0008.

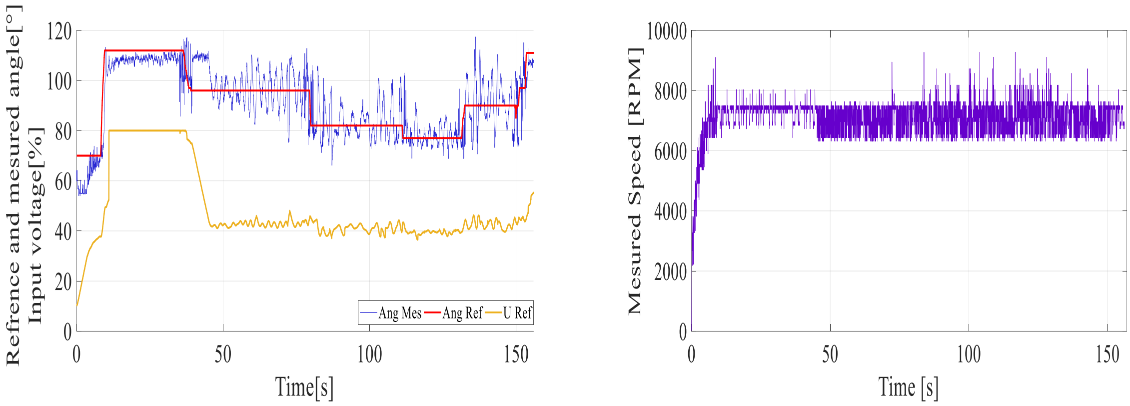

Figure III. 20: Measured speed and reference of angle in a 0.020 and 0.0010.

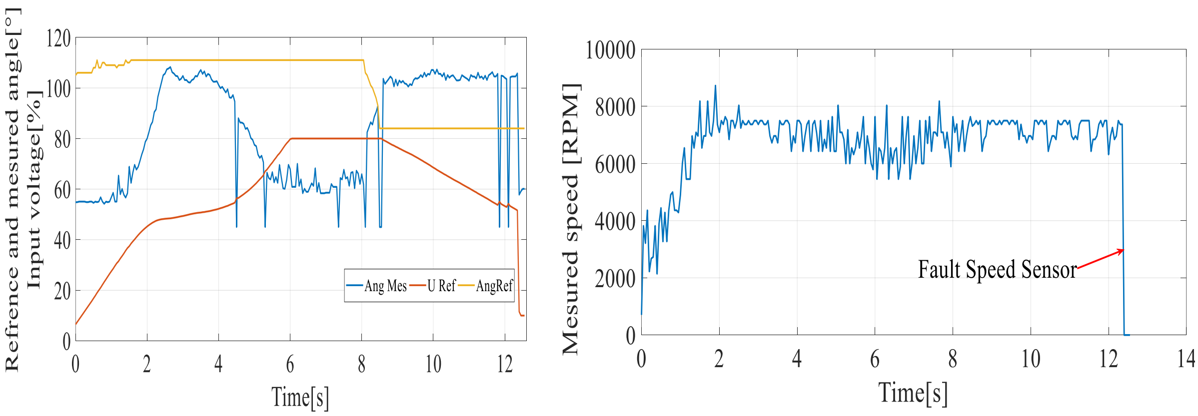

Figure III. 21: Measured speed and reference of angle in a 0.020 and 0.01.

Figure III.21 shows the real time result of angle control for the different parameter Ki, K_p . In order to investigate the performance of the K_p and K_i factor for the angle, voltage, and the speed as shown in Figure (III.17) to Figure (III.21), when K_p and K_i increased it can be seen that the angle measured is not tracking the reference angle, that means the voltage reference and the speed also changed.

Thank to data Simulink the better value has been applied to experimental real time test.

As represented in figure K_i =0.007 and K_p=0.003.

- **Voltage and current for dynamic control**

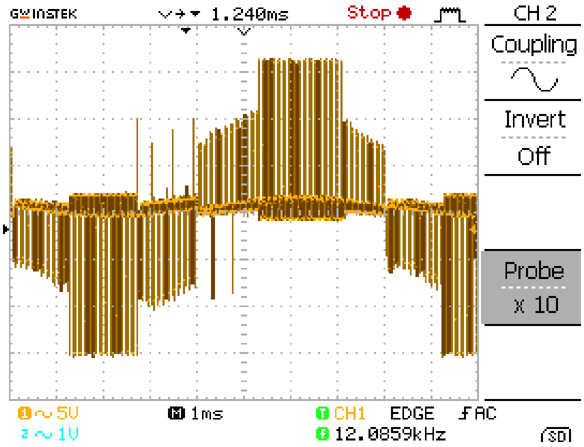

Composed voltage

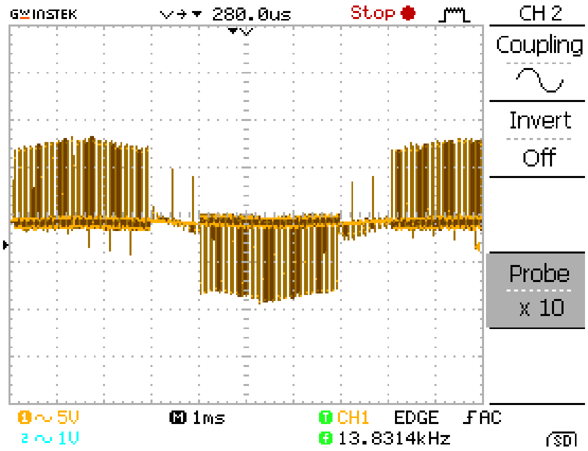

Simple voltage

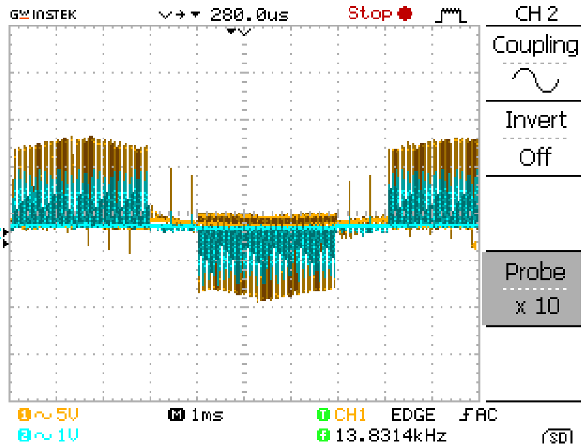

Simple Voltage and current changes

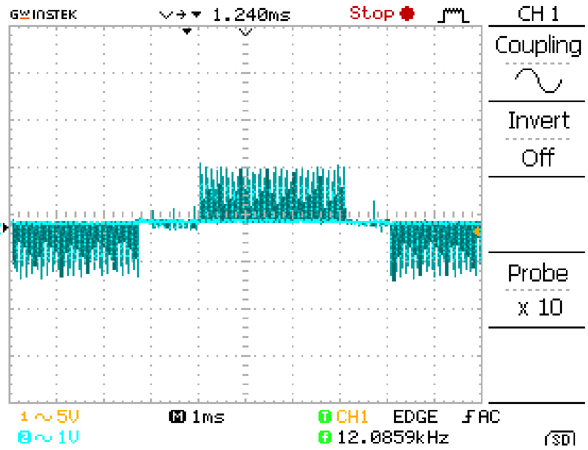

Curent

Figure III. 22: Diagram of Voltage and current changes at 2500rpm.

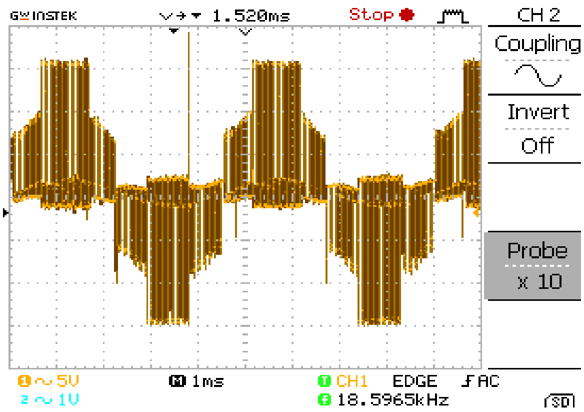

Composed voltage

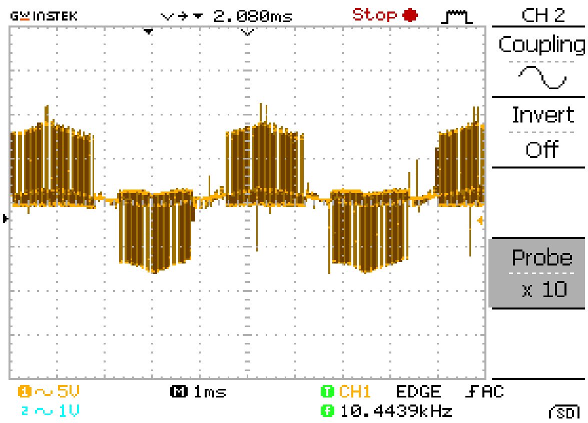

Simple voltage

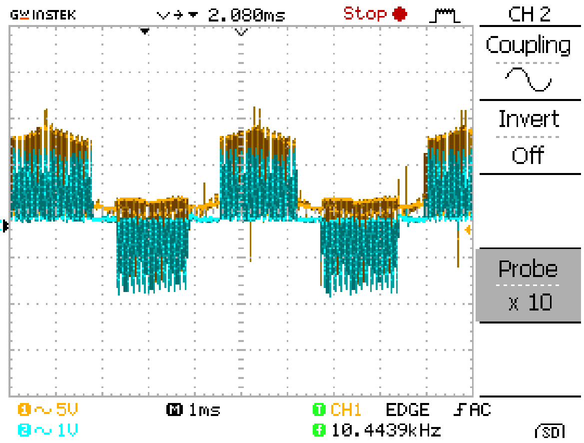

Simple Voltage and current changes

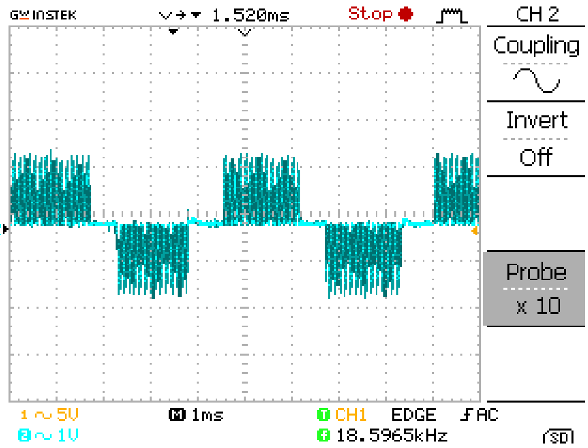

Curent

Figure III. 23: Diagram of Voltage and current changes at 4000rpm.

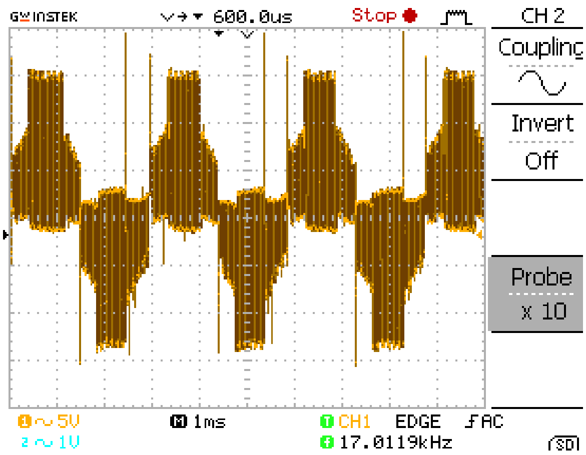

Composed voltage

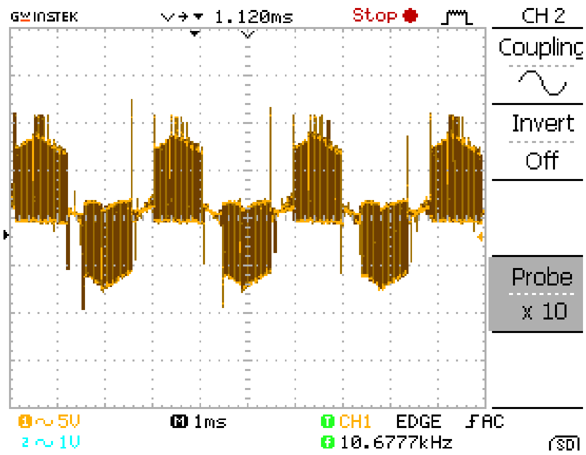

Simple voltage

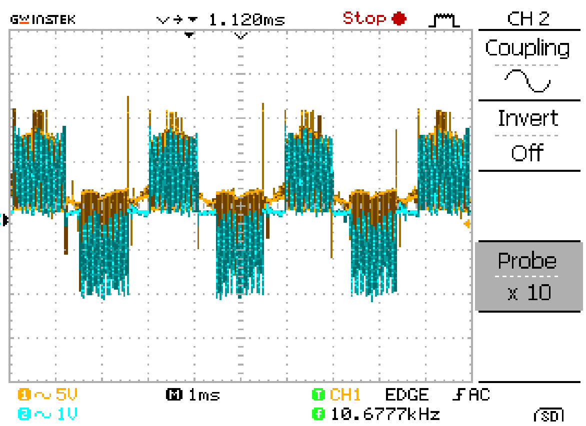

Simple Voltage and current changes

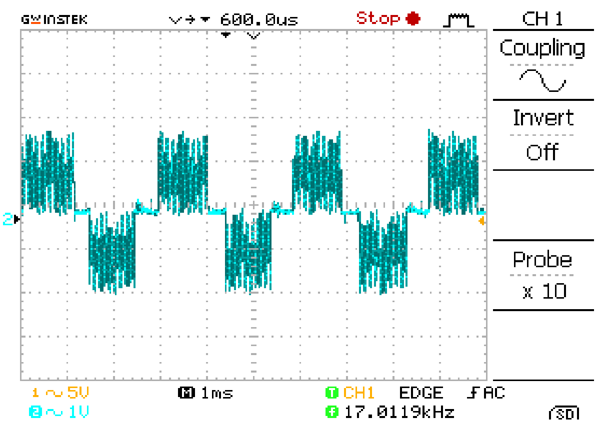

Curent ligne

Figure III. 24: Diagram of Voltage and current changes at 6000rpm.

Figures (III.21, 22, 23, 24, 25) represent the real time results of voltage and current at speed 2500 rpm, 4000 rpm,6000rpm, respectably.

According the presented results we can notes that at speed rpm the period T_p=8ms, so frequency $f_r = \frac{1}{8} \times 10^3 = 125\ Hz$, Also for the current and voltage at speed 4000 rpm, $T_s = \frac{1}{4.5} \times 10^3$so frequency $f_r = 222.2\ Hz$,and at speed 6000 2500 rpm the frequency $f_r = \frac{1}{3} 10^3 = 333\ Hz.$

From this result, we control the result between the speed and the frequency from the result on the speed $= \frac{f}{P_s}$,P_s: number the pole.

III.7 Conclusion

In this chapter, the data model of the BLDC motor based on exprimental test for the simulation model of the mechanical and electrical system has been devlopped .Other wise, the real time speed and angle control has been acheved by using PI regulotor. Hence, the optimum pramater Ki ,Kp tested in simulink model apluied on real time controller.

The object of angle and speed control is the dynamic stabilisation of one axe in quadcopter and maybe applied for the other axes.

Finally, the results of voltage, current speed and angle in real time has been presented for different situations of regulator parameters ki, kp. The last results approve the effectivenesse and validity of realised system.

General conclusion

General conclusion

Quad-copter is an unmanned aerial vehicle (UAV) or drone with four rotors, each with a motor and propeller. A quad-copter can be manually controlled or can be autonomous. It's also called quad-rotor helicopter or quad-rotor.

Firstly, we basic principles of quad -copter design as well as current applications are represented. Quad-copter could be used for safety inspections, perimeter patrols around prisons and thermal imaging to check for cannabis being grown in roof lofts and other not easy to access locations. Future research will be in field of search and rescue. In future, an effort will be directed to development of a system for defining evacuation/safe path in case of natural disasters and accidents. The system will consists of quad-copter, which is equipped with a camera to capture different terrain (land or water) and a processing unit for processing the recorded Condi it is possible to use this system in cases of climatic changes that affect the safety and health of the population or in cases where it is endangering the functionality of different economic systems.

In second chapter, we builted the structure successfully using the selected components, and The structure Simulink model was made, based on derived differential equations of motion. The mathematical model of BLDC with inverter was developed and implemented in Simulink for it will be ready to implementation on the real hardware to control of one axe of drone. The structure was built successfully using the selected components, compatible with each other. The structure Simulink model was made, based on derived differential equations of motion. A PI-based controller was designed and tuned for speed control based on reference voltage. The results of proposed strategy confirm the effectiveness of proposed control for applied in real time.

The third chapter ,we presented the data model of the BLDC motor based on experimental test for the simulation model of the mechanical and electrical system has been developed and the real time speed and angle control has been achieved by using PI regulator. Hence, the optimum parameter Ki, Kp tested in Simulink model applied on real time control.

Finally, we conclude the effect of parameter Ki, Kp regulator PI is very important for dynamic stabilization in speed and angle control. Then, we propose perspectives for continuing this work for stabilization of quad-copter by using advanced controller.

References

References:

Uncategorized References

1. Benhamou, P., et al., *Intitulé du sujet Réalisation d'un drone Quad-copter*. 2018.
2. Vergouw, B., et al., *Drone technology: Types, payloads, applications, frequency spectrum issues and future developments*, in *The future of drone use*. 2016, Springer. p. 21-45.
3. Elijah, T., et al., *A review on control and maneuvering of cooperative fixed-wing drones.* International Journal of Dynamics and Control, 2021. **9**(3): p. 1332-1349.
4. Dileep, M., et al. *A study and analysis on various types of agricultural drones and its applications*. in *2020 Fifth International Conference on Research in Computational Intelligence and Communication Networks (ICRCICN)*. 2020. IEEE.
5. kalpa Gunarathna, J. and R. Munasinghe. *Development of a quad-rotor fixed-wing hybrid unmanned aerial vehicle*. in *2018 Moratuwa Engineering Research Conference (MERCon)*. 2018. IEEE.
6. Gamazo-Real, J.C., E. Vázquez-Sánchez, and J. Gómez-Gil, *Position and speed control of brushless DC motors using sensorless techniques and application trends*. sensors. Vol. 10. 2010. 6901-6947.
7. Rahman, M., et al. *Implementation of quadcopter as a teaching tool to enhance engineering courses*. in *2016 IEEE 8th International Conference on Engineering Education (ICEED)*. 2016. IEEE.
8. Kurochkin, V., *Cluster Analysis in agricultural decision support systems development.* Proceedings of the National aviation university, 2016(3): p. 62–68-62–68.
9. Ventura, D., et al., *A low-cost drone based application for identifying and mapping of coastal fish nursery grounds.* Estuarine, Coastal and Shelf Science, 2016. **171**: p. 85-98.
10. Lee, S. and Y. Choi, *Reviews of unmanned aerial vehicle (drone) technology trends and its applications in the mining industry.* Geosystem Engineering, 2016. **19**(4): p. 197-204.
11. Noor, F., et al., *A Review on Communications Perspective of Flying Ad-Hoc Networks: Key Enabling Wireless Technologies, Applications, Challenges and Open Research Topics.* Drones, 2020. **4**(4): p. 65.
12. Sultan, S., et al., *Emergency Aerial Assistance using Quadcopter*. 2014.
13. Ahirwar, s., et al., *Application of Drone in Agriculture.* International Journal of Current Microbiology and Applied Sciences, 2019. **8**: p. 2500-2505.
14. Shahmoradi, J., et al., *A Comprehensive Review of Applications of Drone Technology in the Mining Industry.* Drones, 2020. **4**(3).
15. Singhal, G., B. Bansod, and L. Mathew, *Unmanned Aerial Vehicle Classification, Applications and Challenges: A Review*. 2018.
16. Ostojic, G., et al., *Design, control and application of quadcopter.* International Journal of Industrial Engineering and Management, 2015. **6**: p. 43-48.
17. Paneque-Gálvez, J., et al., *Small Drones for Community-Based Forest Monitoring: An Assessment of Their Feasibility and Potential in Tropical Areas.* Forests, 2014. **5**(6).
18. Shaaban, G., et al., *introduction To Quadcopters.* 2016.
19. Baldursson, S., *Bldc motor modelling and control-a matlab®/simulink® implementation*. 2005.
20. Muniraj, M. and R. Arulmozhiyal, *Investigation on modeling and simulation BLDC motor fed universal actuation system.* Revista Internacional de Métodos Numéricos para Cálculo y Diseño en Ingeniería, 2020. **36**.
21. Kim, S.-H., *Chapter 10 - Brushless direct current motors*, in *Electric Motor Control*, S.-H. Kim, Editor. 2017, Elsevier. p. 389-416.
22. Kim, S.-H., *Brushless direct current motors*. 2017. p. 389-416.
23. Tsai, M.-F., et al. *Model construction and verification of a BLDC motor using MATLAB/SIMULINK and FPGA control*. in *2011 6th IEEE Conference on Industrial Electronics and Applications*. 2011. IEEE.

24. Åström, K.J., K.H. Johansson, and Q.-G. Wang *Design of decoupled PI controllers for two-by-two systems*. IEE Proceedings - Control Theory and Applications, 2002. **149**, 74-81.